Thieme

Phyllobilins – Bioactive Natural Products Derived from Chlorophyll – Plant Origins, Structures, Absorption Spectra, and Biomedical Properties

Authors
Cornelia A. Karg[1], Masahiko Taniguchi[2], Jonathan S. Lindsey[2], Simone Moser[1]

Affiliations
1 Department of Pharmacy, Pharmaceutical Biology, Ludwig-Maximilian University of Munich, Germany
2 Department of Chemistry, North Carolina State University, Raleigh, USA

Key words
Bioactivity, chlorophyll catabolites, micronutrients, phyllobilins, phytochemicals, spectral database

received June 27, 2022
accepted after revision September 4, 2022
published online December 8, 2022

Bibliography
Planta Med 2023; 89: 637–662
DOI 10.1055/a-1955-4624
ISSN 0032-0943

Georg Thieme Verlag KG, Rüdigerstraße 14, 70469 Stuttgart, Germany

Correspondence
Dr. Simone Moser
Department of Pharmacy, Pharmaceutical Biology, Ludwig-Maximilian University of Munich
Butenandtstr. 5–13, 81377 Munich, Germany
Phone: + 49 89 2180 77175, Fax: + 49 89 2180 77170
Simone.moser@cup.uni-muenchen.de

ABSTRACT

Phyllobilins are open-chain products of the biological degradation of chlorophyll *a* in higher plants. Recent studies reveal that phyllobilins exert anti-oxidative and anti-inflammatory properties, as well as activities against cancer cells, that contribute to the human health benefits of numerous plants. In general, phyllobilins have been overlooked in phytochemical analyses, and – more importantly – in the analyses of medicinal plant extracts. Nevertheless, over the past three decades, > 70 phyllobilins have been identified upon examination of more than 30 plant species. Eight distinct chromophoric classes of phyllobilins are known: phyllolumibilins (PluBs), phylloleucobilins (PleBs), phylloxanthobilins (PxBs), and phylloroseobilins (PrBs)–each in type-I or type-II groups. Here, we present a database of absorption and fluorescence spectra that has been compiled of 73 phyllobilins to facilitate identification in phytochemical analyses. The spectra are provided in digital form and can be viewed and downloaded at www.photochemcad.com. The present review describes the plant origin, molecular structure, and absorption and fluorescence features of the 73 phyllobilins, along with an overview of key medicinal properties. The review should provide an enabling tool for the community for the straightforward identification of phyllobilins in plant extracts, and the foundation for deeper understanding of these ubiquitous but underexamined plant-derived micronutrients for human health.

Introduction

The green plant pigments chlorophyll *a* and chlorophyll *b* are vital cofactors for life on Earth. In addition to their essential roles in photosynthesis, chlorophylls *a*/*b* are also efficient photosensitizers of singlet oxygen. In this regard, unused chlorophylls upon release from their binding proteins are harmful to the plant and are converted to phyllobilins [1]. Hendry and coworkers [2] pointed out in 1987 that "it is unfortunate that many scientists as well as laymen hold the quite erroneous belief that the red and orange pigments, characteristic of leaf senescence and crop ripening, are chlorophyll degradation products". Their paper was entitled "The degradation of chlorophyll – a biological enigma" and referred to the unknown fate of an estimated 1000 million metric tons (10^{12} kg) of chlorophylls *a*/*b* per year. Since then, extensive research has yielded an emerging picture of an enzymatically controlled break-

ABBREVIATIONS

COX	cyclooxygenase
DNCC	dioxobilin-type non-fluorescent chlorophyll catabolite
DPiCC	dioxobilin-type pink chlorophyll catabolite
DPleB	dioxobilin-type phylloleucobilin (type-II)
DPluB	dioxobilin-type phyllolumibilin (type-II)
DPrB	dioxobilin-type phylloroseobilin (type-II)
DPxB	dioxobilin-type phylloxanthobilin (type-II)
DYCC	dioxobilin-type yellow chlorophyll catabolite
*hm*PluB	hypermodified phyllolumibilin (type-I)
*m*PluB	modified phyllolumibilin (type-I)
NCC	non-fluorescent chlorophyll catabolite
PAO	pheophorbide *a* oxygenase
*p*FCC	primary fluorescent chlorophyll catabolite
PiCC	pink chlorophyll catabolite
PleB	phylloleucobilin (type-I)
PluB	phyllolumibilin (type-I)
*p*PluB	primary phyllolumibilin (type-I)
PrB	phylloroseobilin (type-I)
PxB	phylloxanthobilin (type-I)
RCC	red chlorophyll catabolite
RCCR	red chlorophyll catabolite reductase
YCC	yellow chlorophyll catabolite

down pathway for chlorophyll that affords intermediate and terminal catabolites, the phyllobilins. Phyllobilins are open-chain structures generated by demagnesiation, dephytylation, and oxygenolytic ring-opening of the chlorophyll *a* macrocycle [3]. In this breakdown pathway, chlorophyll *b* is converted to chlorophyll *a* and, hence, is also funneled into the same catabolic process [4].

Phyllobilins are now believed to be ubiquitous in nature, as evidenced by the identification of > 70 phyllobilins from more than 30 plant species [5]. The known phyllobilins encompass rich structural diversity and constitute a previously unexplored class of natural products. All phyllobilins contain the five rings (A–E) derived from chlorophyll *a* but differ in (1) path of conjugation, (2) composition of terminal rings A and D, (3) stereochemical configuration at four or more sites, and (4) presence of a range of substituents at multiple sites (▶ **Fig. 1**). The structural diversity, distinct variations across plants, and range of light absorption (from colorless to colored) have presented challenges to the identification and development of a coherent picture concerning the origin of phyllobilins. The analytical challenges associated with fractionation, identification and characterization of phyllobilins indeed are acute, as illustrated by a chromatogram of a plant extract shown in ▶ **Fig. 2**.

Beyond the challenges of a kaleidoscope of structural variety, phyllobilins have suffered from entrenched biochemical dogma – that catabolic products are mere throw-away byproducts and consequently warrant little interest. In this view, phyllobilins as non-photosensitizers would solely be the detoxified waste products of chlorophylls. Studies in the past three decades have overturned this dogma and revealed phyllobilins to constitute a rich

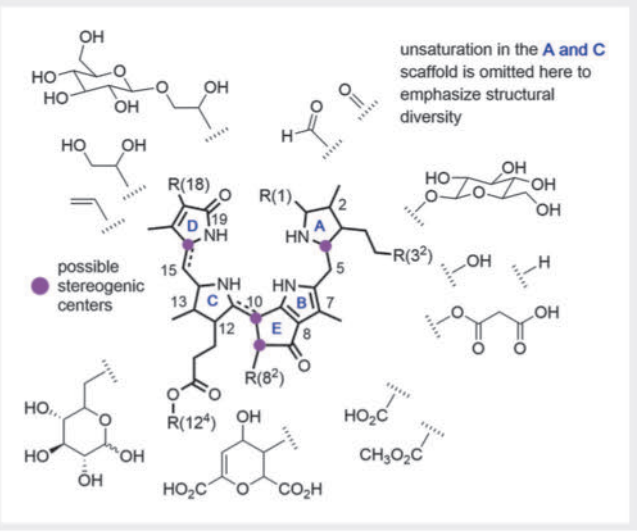

▶ **Fig. 1** Phyllobilin structural diversity. Phyllobilins differ structurally in peripheral modifications at R(1), R(3^2), R(8^2), R(12^4), R(18) (examples are shown), stereochemical configuration and number of stereogenic centers, assembly of rings A and D, and saturation level (not complete).

class of natural products with diverse and beneficial bioactivities [5]. Thus, phyllobilins are potent antioxidants and are now known to exhibit anti-inflammatory activities, as well as anti-proliferative effects on cancer cells at such a level in human cells as to be considered valuable micronutrients in plant-based diets. The bioactivities of selected phyllobilins may account for the human health-promoting effects of certain herbal remedies and medicinal plants [7, 8]. Possible biological roles for phyllobilins in plants, other than the absence of photosensitization properties characteristic of the antecedent chlorophylls, are not yet clear but also have hardly been explored.

In Munich, we have been working to understand the biomedical effects of phyllobilins. In Raleigh, we have been working to assemble and organize spectral data for important chromophores and pigments to advance the photochemical sciences. In this paper, we combine our research interests in the assembly of a database of absorption and fluorescence spectra of 73 phyllobilins. These 73 structures represent the family of phyllobilins with regard to their spectral properties, as distinct classes of phyllobilins exhibit characteristic spectral features; among them are naturally occurring examples, as well as synthetically generated structures. For comparative purposes, the spectra of a small set of additional chromophores that constitute the core components of various phyllobilins are also presented. The spectra along with structures and literature citations are available for downloading at no cost at www.photochemcad.com.

The present review is aimed at multiple audiences within the wide scope of the plant sciences. A broad audience may be interested in the overview of the plant origins, structures, and biomedical properties of phyllobilins. Scientists engaged in fractionating plant extracts may find the database of spectra for 73 phyllobilins, which have not previously been assembled, of use for assessing the purity of phyllobilins. The tabulated effects of conjugation

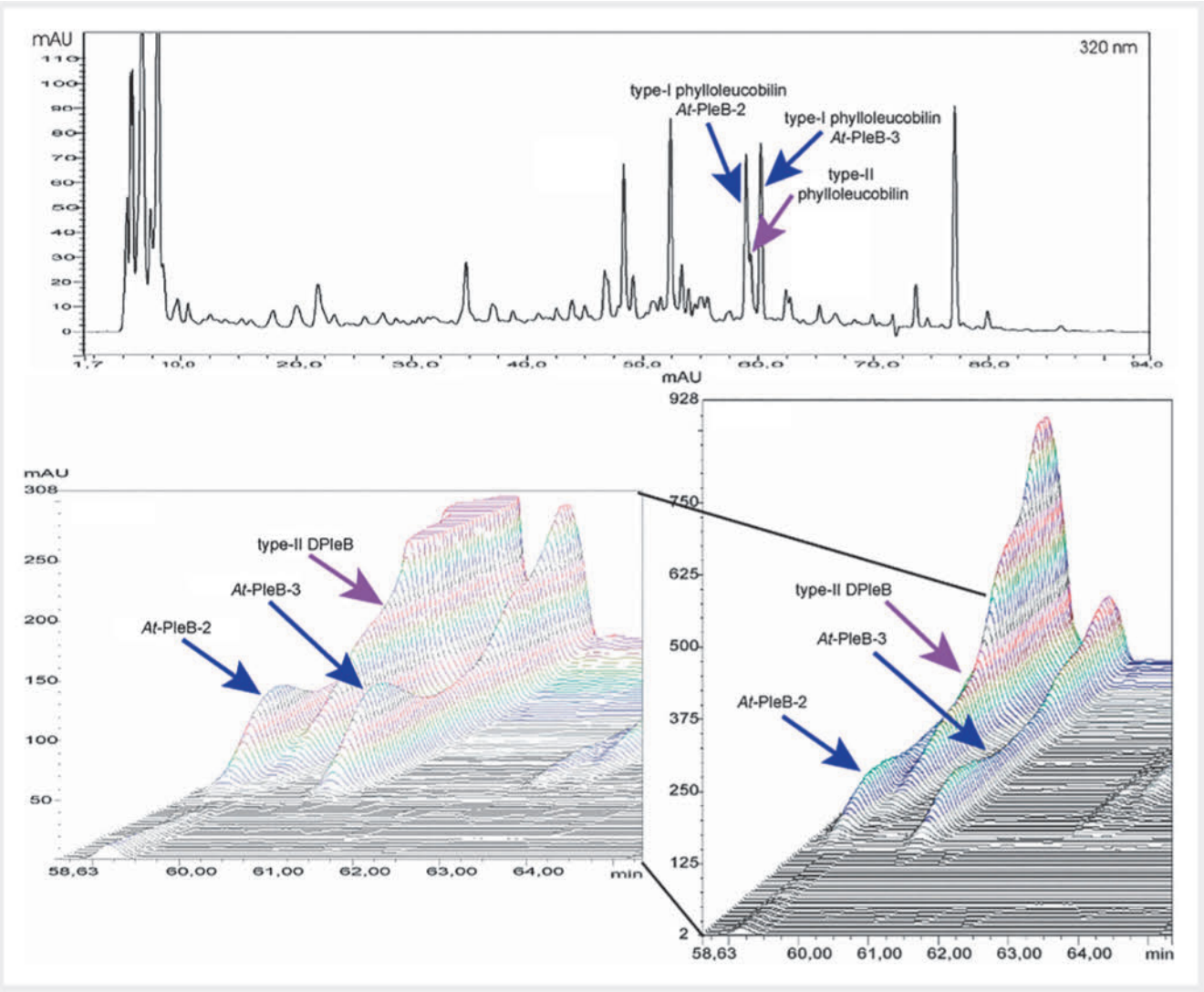

▶ **Fig. 2** HPL-chromatogram of an extract of senescent leaves of *Arabidopsis thaliana*, detected at 320 nm (upper panel, solvent system: methanol and PPB, pH 7). 3D-field spectrum of the chromatogram between 58.6 min and 65.3 min (right bottom panel, zoom in at the left bottom panel). The chromatogram and corresponding 3D-field spectral analysis illustrate the importance of analyzing the entire wavelength spectrum of HPL-chromatograms for the identification of different phyllobilin species, since type-II phyllobilins are often missed when detecting at 320 nm (figure adapted from [6]).

and substituents on spectral properties, including comparison with simpler components, may intrigue those with a fundamental or educational inclination. For biomedical studies of phyllobilins, the database may enable a rapid assessment of sample purity and type. Taken together, the review provides a comprehensive overview of the spectra of all known phyllobilins along with insights concerning their plant origin, structure, and properties.

Reconnaissance – Plant Origin of Phyllobilins

The biochemical program of chlorophyll breakdown is named after pheophorbide *a* oxygenase (PAO), the key enzyme responsible for the linearization of the chlorin macrocycle, and the end-products, the phyllobilins [3]. In the first steps of the PAO/phyllobilin pathway, chlorophyll *a* is converted to a red chlorophyll catabolite (RCC), which is further metabolized in an enzyme-bound form to a 'primary' fluorescent chlorophyll catabolite (*p*FCC), also termed a phyllolumibilin (*p*PluB) (▶ **Fig. 3**) [9, 10]. The responsible enzyme, the RCC reductase (RCCR), reduces the double bond of the RCC at C15/C16 stereospecifically to form *p*PluBs of the '*n*' or '*epi*' type, depending on the plant species [11]. A given plant typically contains one RCCR; hence, the resulting *p*PluB has a particular stereochemical configuration at position C16; the absolute configuration, however, has not been determined yet.

Following enzymatic formation of the phyllolumibilin, three pathways ensue (▶ **Fig. 4**). In one path, the *p*PluB is transformed by enzymes to 'modified' PluBs (*m*PluBs) that retain the characteristic formyl group at ring A (type-I phyllobilins). In a second path, the *p*PluB undergoes oxidative deformylation by a cytochrome-P_{450} enzyme to yield dioxobilin-type phyllolumibilins (DPluBs) that

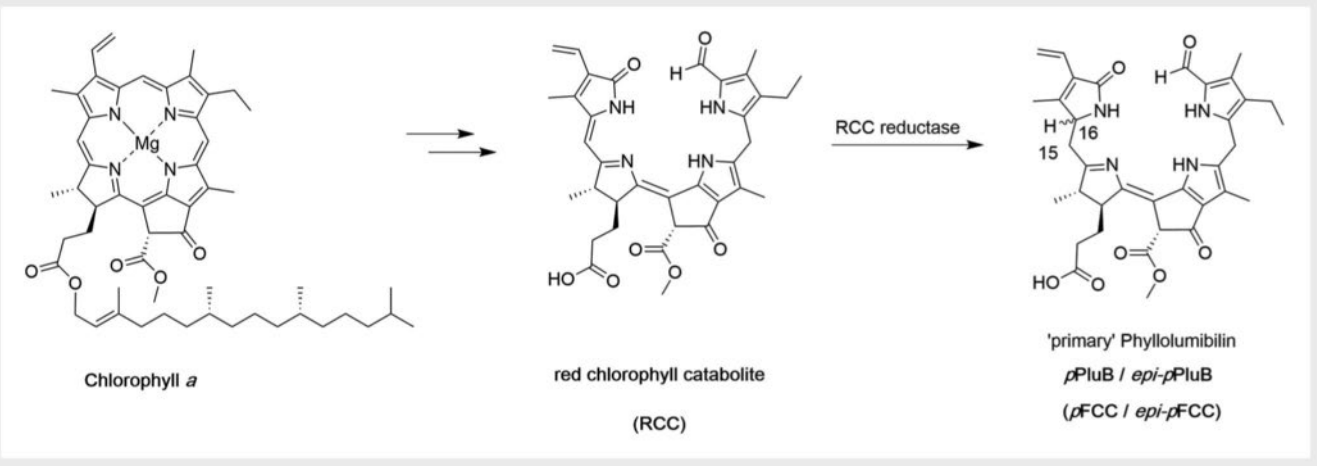

▶ **Fig. 3** Early stages of chlorophyll breakdown – demetalation, dephytylation, and oxygenolytic opening of the macrocycle (catalyzed by PAO) to form RCC. Reduction of the C15/C16 double bound of RCC by RCCR affords the 'primary' phyllolumibilin (*p*PluB, formerly *p*FCC) containing a new stereocenter at C16 in either the '*n*' or '*epi*' configuration [11].

▶ **Fig. 4** Overview of the three known branches of late chlorophyll breakdown. The *p*PluB or its C16-isomer *epi-p*PluB are transformed in three possible pathways: forming type-I phyllobilins (left panel), type-II phyllobilins (middle panel), and hypermodified phyllolumibilins (right panel). The scope of R groups is described in the following text.

feature a γ-lactam group at ring A (type-II phyllobilins) [12]. (Note that the prefix "D" is added to indicate "dioxo" and is synonymous with the label "type-II".) Although PluBs are fleeting intermediates because of rapid metabolism, in some cases a third path affords stabilized hypermodified phyllolumibilins (*hm*PluBs). The hypermodified PluBs are formed by esterification at the propionic acid side chain, which renders the PluBs more persistent and therefore detectable and isolable [13]. In all three routes, *p*PluBs are modified by the introduction of hydrophilic peripheral residues.

The *m*PluBs and DPluBs are non-enzymatically converted to non-fluorescent chlorophyll catabolites (NCCs and DNCCs), also called phylloleucobilins (PleBs and DPleBs) (▶ **Fig. 4**). The latter accumulate in the vacuoles of the plant cells and to date are the best-characterized phyllobilin structures [14]. As their name implies, the phylloleucobilins are not colored. However, the phylloleucobilins can be oxidized by a still elusive 'oxidative activity' to colored pigments, the yellow chlorophyll catabolites (YCCs and DYCCs), also known as phylloxanthobilins (PxBs and DPxBs) [15–17]. The phylloxanthobilins and phylloleucobilins differ only in the position of a single double bond (▶ **Fig. 4**).

PxBs can – at least chemically – be further oxidized to form pink chlorophyll catabolites (PiCC and DPiCC) or phylloroseobilins (PrBs and DPrBs) (▶ **Fig. 4**) [18–20]. PrBs have so far only been detected in minute amounts in plant extracts [18, 21]; the structure of a DPrB has not been identified in plants but was generated by synthetic approaches [20]. In sum, a striking feature of the chlorophyll catabolic pathway is the interspersion of oxidation and reduction reactions: chlorophyll *a* to PluBs (oxidation), conversion to PleBs (reduction), conversion to PxBs (oxidation), and conversion to PrBs (oxidation). Since these yellow (PxBs) and pink (PrB) phyllobilins possess photoactive properties and decreased polarity, their presence clearly contradicts the detoxification paradigm of the biochemical program of chlorophyll degradation.

Phyllobilin Structures and Nomenclature

The previous section shows the existence of parallel terminology for phyllobilins. The original names were given in terms of plant origin, physical properties, and molecular structure. The term 'phyllobilin' was introduced in 2014, reflecting the origin from chlorophyll and the structural similarity to the heme-derived bilins [3, 22]. The structure of a type-II phylloxanthobilin is analogous to that of bilirubin, whereas a type-II phylloroseobilin is analogous to that of biliverdin (▶ **Fig. 5**). The phyllobilins contain rings A–E, whereas bilins (bilirubin, biliverdin) contain only four rings, lacking the isocyclic ring (ring E) characteristic of chlorophylls.

Phyllobilins are now known to encompass considerable diversity with regards to the chromophore and the peripheral substituents [5]. With respect to their physical properties, fluorescent chlorophyll catabolites (FCCs and DFCCs) are now called phyllolumibilins (PluBs and DPluBs), non-fluorescent chlorophyll catabolites (NCCs and DNCCs) are now referred to as phylloleucobilins (PleBs and DPleBs), yellow catabolites are termed phylloxanthobilins (PxBs and DPxBs), and pink pigments are called phylloroseobilins (PrBs and DPrBs). Phyllobilin structures identified from different plant species are usually named with the initials of the botanical name of the plant source as a prefix, the type of the phyllobilin core structure, and a number indicating the polarity in reversed-phase chromatography or a consecutive number [23], e.g., *Ep-*

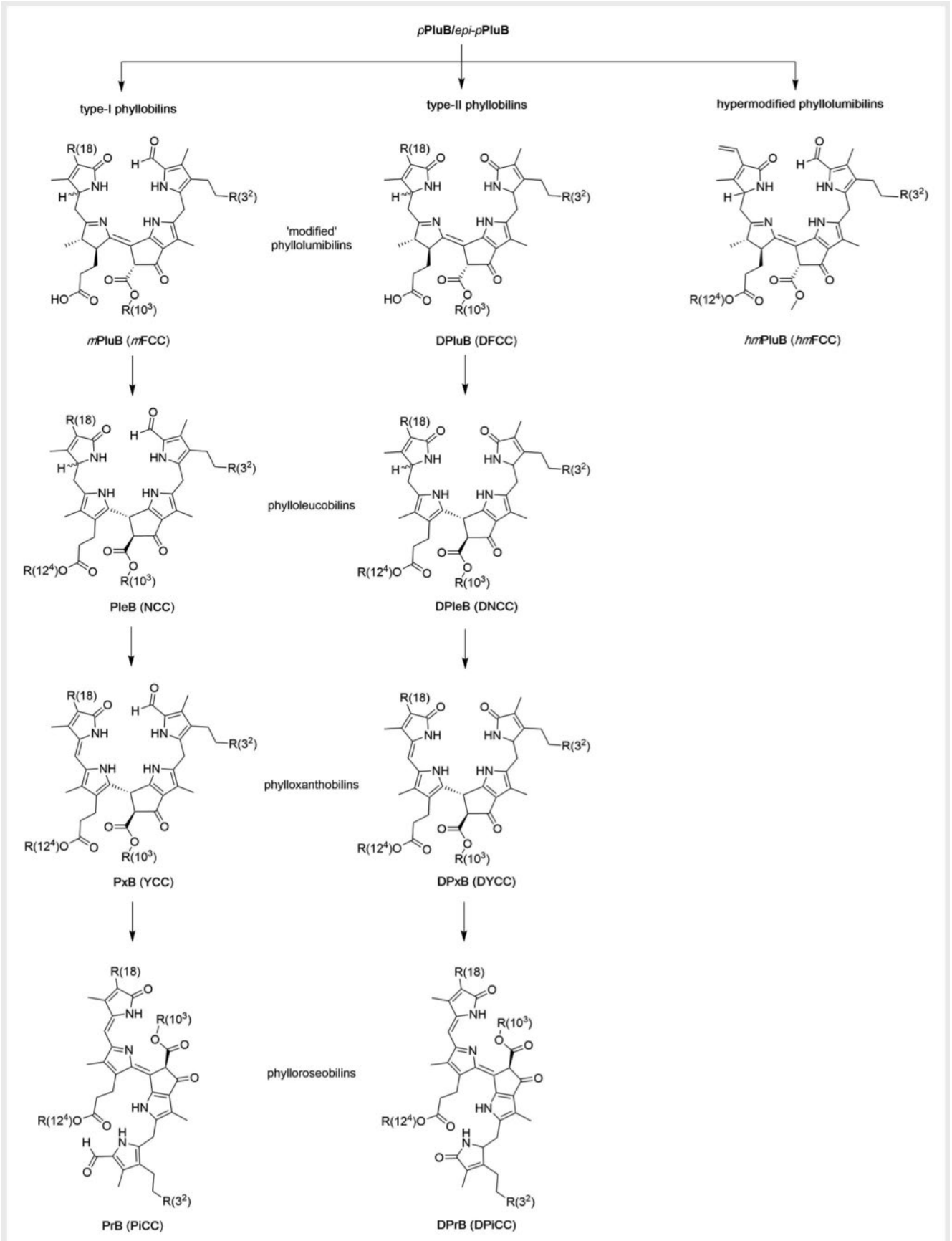
pPluB/epi-pPluB
type-I phyllobilins
type-II phyllobilins
hypermodified phyllolumibilins
'modified' phyllolumibilins
mPluB (mFCC)
DPluB (DFCC)
hmPluB (hmFCC)
phylloleucobilins
PleB (NCC)
DPleB (DNCC)
phylloxanthobilins
PxB (YCC)
DPxB (DYCC)
phylloroseobilins
PrB (PiCC)
DPrB (DPiCC)

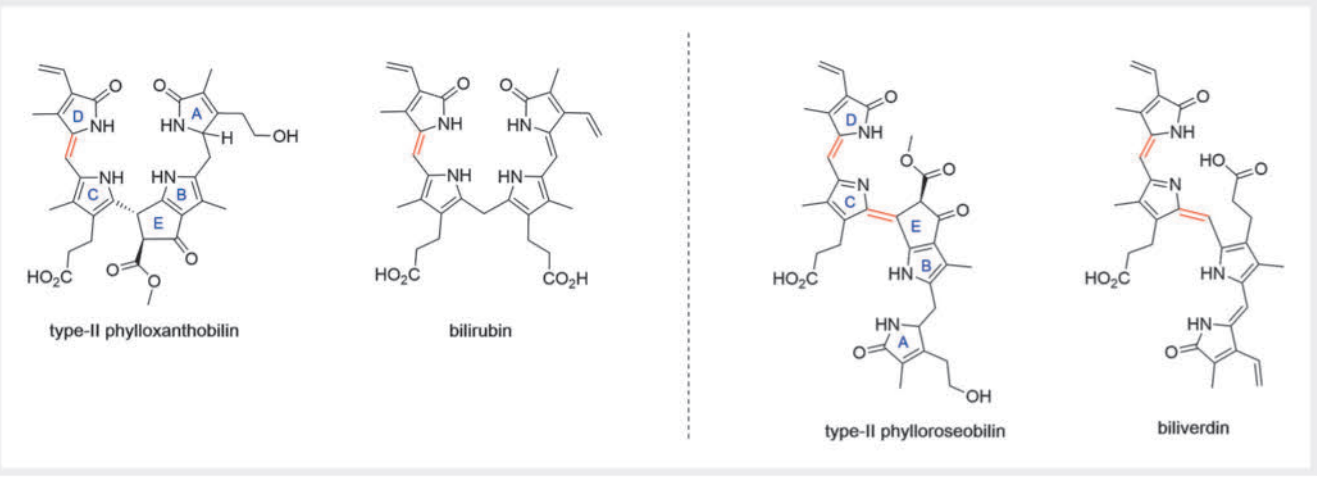

▶ **Fig. 5** Comparison of phyllobilins and bilins, derived from chlorophyll *a* and heme, respectively.

PxB-1 to *Ep*-PxB-6 for the PxBs isolated from senescent leaves of *Echinacea purpurea* [8]. ▶ **Table 1** contains information for 73 phyllobilins of diverse plant origin and structure. The plants of origin shown here include apple (*Malus domestica*), apricot (*Prunus armenica* L.), banana fruits (*Musa cavendish*), basil (*Ocimum basilicum*), broccoli (*Brassica oleracea var italica*), chili pepper (*Capsicum anuum*), grapevine (*Vitis vinifera*), katsura tree (*Cercidiphyllum japonicum*), money plant (*Epipremnun aureum*), mouse-ear cress (*Arabidopsis thaliana*), Norway maple (*Acer platanoides*), plum (*Prunus x domestica*), red cornflower (*Echinacea purpurea*), savoy cabbage (*Brassica oleracea var sabauda*), and wych elm (*Ulmus glabra*). Column 1 of ▶ **Table 1** provides a unique number for each phyllobilin. The new terms and the legacy terms are presented in ▶ **Table 1**, columns 2 and 3, respectively. The numbering of substituents is provided in ▶ **Fig. 4**. Structures of all 73 phyllobilins are illustrated in ▶ **Fig. 6**. The organization of the phyllobilins in ▶ **Table 1** and **Fig. 6** is on the basis of structural class.

Spectral Data and Features

The spectral data for the 73 phyllobilins listed in ▶ **Table 2** and depicted in ▶ **Fig. 2** were obtained from digital files acquired in the laboratory of one of us (S. M.), or by digitization of spectra in the print literature. The process of digitization has been described in detail [49]. All spectra presented herein are available for viewing and/or downloading at no cost at the website www.photochemcad.com. The PhotochemCAD initiative is aimed at assembling spectral data for diverse compounds in an effort to advance the photosciences. The PhotochemCAD program contains a suite of modules for carrying out diverse photophysical calculations [50] along with spectral databases. Collections of spectral data are of most value when curated in an organized fashion and connected with the originating scientific literature [51], as has been done here. The phyllobilins' spectral data complement those already available for 300 common compounds [52], 150 chlorophylls and derivatives [49], > 400 synthetic chlorins [53], and 16 tolyporphins [54].

The spectral parameters of the 73 phyllobilins are provided in ▶ **Table 2**. The table includes the unique number of each phyllobilin (column 1), the new names (column 2), solvent (column 3), absorption maxima and relative intensity (column 4), molar absorption coefficients where available (column 5), fluorescence maxima and fluorescence quantum yield values where available (column 6), and literature references (column 7). The relative intensity of the absorption maximum of a given spectrum is set relative to the most intense peak in the region > 200 nm. The tiny quantities of some phyllobilins isolated following laborious extraction and fractionation from plants has generally precluded determination of molar absorption coefficients.

The absorption spectra are displayed in ▶ **Fig. 7**. The absorption spectra of type-I phyllobilins are shown in panels 1–4, whereas type-II phyllobilins are shown in panels 5–8. An individual panel contains all available spectra of a given chromophore class. Thus, for type-I phyllobilins, PluBs are shown in panel 1, PleBs in panel 2, PxBs in panel 3, and PrB and its metal complexes in panel 4. The same organization holds for the type-II phyllobilins in panels 5–8.

The absorption spectra of phyllobilins of a given category are nearly identical with each other as described in the following.

- The absorption spectra of PluBs **2–7** consist of two peaks at ~ 317 nm and ~ 360 nm (relative intensity ~ 0.7). While absorption < 230 nm was not reported, a band should appear at ~ 215 nm by analogy with the absorption spectra of other phyllobilins (▶ **Fig. 7**, panel 1). The absorption spectrum of DPluB **52** contains two peaks (217 and 361 nm) with a shoulder at 247 nm (▶ **Fig. 7**, panel 5).
- The absorption spectra of PleBs **8–25** exhibit two major peaks (at ~ 215 and ~ 315 nm; relative intensity ~ 0.65) with a shoulder at ~ 243 nm (▶ **Fig. 7**, panel 2). The absorption spectra of DPleBs **55–63** show only one major peak ~ 215 nm with shoulders at ~ 245 and ~ 285 nm (▶ **Fig. 7**, panel 6).
- The absorption spectra of PxBs **26–42** comprise four major peaks (at ~ 215, ~ 247, ~ 312, and 415 to 438 nm), and the longest wavelength peaks (415 to 438 nm) of *E* isomers are bathochromically shifted by ~ 10 nm compared to those of the corresponding *Z* isomers (▶ **Fig. 7**, panel 3).

▶ **Table 1** Structures of phyllobilins (for labels R(X) and C16 see ▶ **Figs. 3** and **4**).

#	Name (new)[a]	Name (original)	R(3^2)	R(10^3)	R(12^4)	R(18)	C16	Reference
1	RCC-Me		H	CH_3	CH_3	$CH{=}CH_2$	–	[24]
Phyllolumibilins (PluBs)								
2	*Ca*-PluB-2	*Ca*-FCC-2	H	CH_3	H	$CH{=}CH_2$	epi	[25]
3	*Mc*-PluB-56	*Mc*-FCC-56	OH	CH_3	5′-daucyl[b]	$CH{=}CH_2$	epi	[13]
4	*Vv*-PluB-55	*Vv*-FCC-55	O-Glc[c]	CH_3	6′-βGlc[c]	$CH{=}CH_2$	epi	[26]
5	At_{mes16}-PluB-1	mes16-FCC-1	O-Glc	CH_3	H	$CH{=}CH_2$	n	[27]
6	*Epa*-PluB		O-Glc	CH_3	–[d]	$CH{=}CH_2$	n. a.	[28]
7	*Mc*-PluB-71	Me–sFCC	OH	CH_3	CH_3[e]	$CH{=}CH_2$	epi	[29]
Phylloleucobilins (PleBs)								
8	*Cj*-PleB-1	*Cj*-NCC-1	OH	CH_3	H	$CH{=}CH_2$	epi	[30]
9	*Po*-PleB		OH	CH_3	H	$CH{=}CH_2$	n	[31]
10	*Cj*-PleB-2	*Cj*-NCC-2	H	CH_3	H	$CH{=}CH_2$	epi	[14]
11	*Md*-PleB-1	*Md*-NCC-1	O-Glc	CH_3	H	$CH{=}CH_2$	epi	[32]
12	*Ob*-PleB-35[f]	*Ob*-NCC-35	O-Mal	CH_3	H	$CH{=}CH_2$	n. a.	[33]
13	*Ob*-PleB-36[g]	*Ob*-NCC-36	O-Mal	CH_3	H	$CH{=}CH_2$	n. a.	[33]
14	*Ob*-PleB-40	*Ob*-NCC-40	O-Mal	CH_3	H	$CH{=}CH_2$	n. a.	[33]
15	*Mc*-PleB-55	*Mc*-NCC-55	OH	CH_3	–[h]	$CH{=}CH_2$	epi	[29]
16	*Mc*-PleB-58	*Mc*-NCC-58	OH	CH_3	–[i]	$CH{=}CH_2$	epi	[29]
17	*Ug*-PleB-53	*Ug*-NCC-53	O-Glc[c]	CH_3	6′-βGlc[c]	$CH{=}CH_2$	epi	[34]
18	*At*-PleB-2	*At*-NCC-2	OH	H	H	$CH{=}CH_2$	n	[35]
19	*At*-PleB-3	*At*-NCC-3	H[j]	H	H	$CH{=}CH_2$	n	[36]
20	*Bo*-PleB-1	*Bo*-NCC-1	O-Glc	H	H	$CH{=}CH_2$	n	[37]
21	*Bo*-PleB-2	*Bo*-NCC-2	H	H	H	$CH{=}CH_2$	n	[37]
22	*Cj*-PleB-Me		OH	CH_3	CH_3	$CH{=}CH_2$	epi	[31]
23	*Cj*-PleB-Et		OH	CH_3	C_2H_5	$CH{=}CH_2$	epi	[31]
24	*Cj*-PleB-Bu		OH	CH_3	C_4H_9	$CH{=}CH_2$	epi	[31]
25	*Cj*-PleB-Oct		OH	CH_3	C_8H_{17}	$CH{=}CH_2$	epi	[31]
Phylloxanthobilins (PxBs)								
26	*Cj*-PxB-2[k]	*Cj*-YCC-2	OH	CH_3	H	$CH{=}CH_2$	–	[16]
27	*Cj*-PxB-1[l]	*Cj*-YCC-1	OH	CH_3	H	$CH{=}CH_2$	–	[18]
28	(*Z*)-*Ep*-PxB-1		O-(6′-OMal)Glc	CH_3	H	$CH(OH)\text{-}CH_2OH$	–	[8]
29	(*Z*)-*Ep*-PxB-2		O-Glc	CH_3	H	$CH(OH)\text{-}CH_2OH$	–	[8]
30	(*Z*)-*Ep*-PxB-3		OH	CH_3	H	$CH(OH)\text{-}CH_2OH$	–	[8]
31	(*Z*)-*Ep*-PxB-4		O-(6′-OMal)Glc	CH_3	H	$CH{=}CH_2$	–	[8]
32	(*E*)-*Ep*-PxB-4		O-(6′-OMal)Glc	CH_3	H	$CH{=}CH_2$	–	this publication
33	(*Z*)-*Ep*-PxB-5	*Md*-YCC-51	O-Glc	CH_3	H	$CH{=}CH_2$	–	[8]
34	(*E*)-*Ep*-PxB-5		O-Glc	CH_3	H	$CH{=}CH_2$	–	this publication
35	(*Z*)-*Pa*-PxB-31	*Pa*-YCC-31	O-Glc	CH_3	H	$CH(OH)\text{-}CH_2O\text{-}Glc$	–	[21]

continued

▶ **Table 1** *Continued*

#	Name (new)[a]	Name (original)	R(3^2)	R(10^3)	R(12^4)	R(18)	C16	Reference
36	(*Z*)-*Epa*-PxB	YCC	O-Glc	CH_3	-[d]	$CH=CH_2$	–	[28]
37	(*Z*)-*Ob*-PxB-45	*Ob*-YCC-45	O-Mal	CH_3	H	$CH=CH_2$	–	[33]
38	*Cj*-PxB-2-Me[m]	Me-YCC	OH	CH_3	CH_3	$CH=CH_2$	–	[38]
39	*Cj*-PxB-1-Me[n]	E1-Me	OH	CH_3	CH_3	$CH=CH_2$	–	[38]
40	(*Z*)-pyPxB	pyYCC	OH	–°	H	$CH=CH_2$	–	[39]
41	(*Z*)-pyPxB-Me	Z4-Me	OH	–°	CH_3	$CH=CH_2$	–	[39]
42	(*E*)-pyPxB-Me	E4-Me	OH	–°	CH_3	$CH=CH_2$	–	[39]
43	Zn-(PxB-Me)$_2$	Zn-(Me-YCC)$_2$	OH	CH_3	CH_3	$CH=CH_2$	–	[40]
44	photodimer of *Cj*-PxB-2-Me		OH	CH_3	CH_3	$CH=CH_2$	–	[38]
45	photodimer of pyPxB-Me		OH	–°	H	$CH=CH_2$	–	[39]
Phylloroseobilins (PrBs)								
46	*Cj*-PrB	*Cj*-PiCC	OH	CH_3	H	$CH=CH_2$	–	[18, 19]
47	Zn-PrB[p]	Zn-PiCC	OH	CH_3	H	$CH=CH_2$	–	[19]
48	Cd-PrB[p]	Cd-PiCC	OH	CH_3	H	$CH=CH_2$	–	[19]
49	Cu-PrB[p]	Cu-PiCC	OH	CH_3	H	$CH=CH_2$	–	[19]
50	Ni-PrB[p]	Ni-PiCC	OH	CH_3	H	$CH=CH_2$	–	[19]
51	Pd-PrB[p]	Pd-PiCC	OH	CH_3	H	$CH=CH_2$	–	[19]
Dioxobilin-type Phyllolumibilins (DPluBs)								
52	*At*-DPluB-33	*At*-DFCC-33	OH	H	H	$CH=CH_2$	n	[41]
53	*Vv*-DPluB-53	*Vv*-DFCC-53	O-Glc[c]	CH_3	6′-βGlc[c]	$CH=CH_2$	epi	[26]
54	At_{mes16}-2HM-*iso*-DPluB[q]	7HM-*iso*-DFCC	H	CH_3	H	$CH=CH_2$	n	[42]
Dioxobilin-type Phylloleucobilins (DPleBs)								
55	*Bo*-DPleB-3	*Bo*-DNCC-3	OH	H	H	$CH=CH_2$	n	[37]
56	*Vv*-DPleB-51	*Vv*-DNCC-52	OH	CH_3	H	$CH=CH_2$	epi	[26]
57	*Ap*-DPleB	*Ap*-DNCC	OH	CH_3	H	$CH(OH)-CH_2OH$	epi	[43]
58	At_{mes16}-DPleB-47	At_{mes16}-DNCC-47	H	CH_3	H	$CH=CH_2$	n	[42]
59	*At*-DPleB-45/ At-DPleB-48[r]	*At*-DNCC-45/ At-DNCC-49	H	H	H	$CH=CH_2$	n	[41]
60	At_{mes16}-4HM-DPleB-44[s]	At_{mes16}-9HM-DNCC-45	H	CH_3	H	$CH=CH_2$	n	[42]
61	*At*-4HM-DPleB-41[s]	*At*-4HM-DNCC-41	H	H	H	$CH=CH_2$	n	[44]
62	At_{mes16}-2HM-*iso*-DPleB-46[q]	At_{mes16}-7HM-*iso*-DNCC-46	H	CH_3	H	$CH=CH_2$	n	[42]
63	*At*-2HM-*iso*-DPleB-43[q]	*At*-2HM-*iso*-DNCC-43	H	H	H	$CH=CH_2$	n	[44]
Dioxobilin-type Phylloxanthobilins (DPxBs)								
64	(*Z*)-*Vv*-DPxB-63	*Vv*-DYCC-63	OH	CH_3	H	$CH=CH_2$	–	[15, 26]
65	(*E*)-*Vv*-DPxB-63	(*E*)-*Vv*-DYCC-63	OH	CH_3	H	$CH=CH_2$	–	[15, 26]
66	(*Z*)-*Bos*-DPxB		OH	H	H	$CH=CH_2$	–	[45]
67	(*E*)-*Bos*-DPxB		OH	H	H	$CH=CH_2$	–	this publication

continued

▶ **Table 1** *Continued*

#	Name (new)[a]	Name (original)	R(3^2)	R(10^3)	R(12^4)	R(18)	C16	Reference
Dioxobilin-type Phylloroseobilins (DPrBs)								
68	DPrB	DPiCC	OH	CH_3	H	$CH{=}CH_2$	–	[20]
69	ZnDPrB[t]	ZnDPiCC	OH	CH_3	H	$CH{=}CH_2$	–	[46]
Others								
70	Pa–*i*PB-45[u]		OH	–[°]	H	$CH{=}CH_2$	n. a.	[47]
71	Pa–*i*PB-55[u]		H	–[°]	H	$CH{=}CH_2$	n. a.	[47]
72	Pa–*i*PB-iminoester[v]		OH	–[°]	H	$CH{=}CH_2$	n. a.	[47]
73	yellow biladiene		OH	–[w]	H	$CH{=}CH_2$	–	[48]

[a] *Ca: Capsicum anuum* (chili pepper); *Mc: Musa cavendish* (banana fruits); *Vv: Vitis vinifera* (grapevine); *At: Arabidopsis thaliana* (mouse-ear cress); *Epa: Epipremnun aureum* (money tree); *Cj: Cercidiphyllum japonicum* (katsura tree); *Md: Malus domestica* (apple); *Ob: Ocimum basilicum* (basil); *Ug: Ulmus glabra* (wych elm); *Bo: Brassica oleracea var italica* (broccoli); *Ep: Echinacea purpurea* (purple coneflower); *Pa: Prunus armenica* L. (apricot); Pd: *Prunus x domestica* (plum); *Ap: Acer platanoides* (Norway maple); *Bos: Brassica oleracea var sabauda* (savoy cabbage); [b] Daucic acid bound at 5′-OH; [c] 1′,6′-Glycopyranosyl bridge attached at O^3 and 12^4; [d] Dihydroxyphenylethyl-glucosyl; [e] Presumably artefact from the methanolysis of persistent FCC daucyl esters; [f] Hydroxy moiety at C15, presumably oxidation product of *Ob*-PleB-40 and precursors of *Ob*-PxB-45; [g] Methoxy moiety at C15, presumably oxidation product of *Ob*-PleB-40 and precursors of *Ob*-PxB-45; [h] Daucyl moiety and S configuration at C10 according to CD spectrum; [i] Daucyl moiety and R configuration at C10; [j] $HOCH_2$ moiety at C2; [k] Z isomer of PxB from *Cercidiphyllum japonicum;* [l] *E* isomer of PxB from *Cercidiphyllum japonicum;* [m] *Z* isomer of PxB-Me from *Cercidiphyllum japonicum;* [n] *E* isomer of PxB-Me from *Cercidiphyllum japonicum;* ° Unsubstituted H_2C8^2; [p] Metal complexes of *Cj*-PrB (Zn = zinc, Cd = cadmium, Cu = copper, Ni = nickel); [q] Hydroxymethyl moiety at C2; [r] Assumed to be C4-stereoisomers; [s] Hydroxylmethyl moiety at C4; [t] Zinc complex of DPrB; [u] Iso-phyllobilanones (iPB), ring A together with C5 methylene group is attached at C7 of ring B, and ring B features a lactam group; [v] Iso-phyllobilanone-iminoester, O-methylated iminoester function at ring B; [w] Product of the cleavage of the peripheral C–C bond of the ring E unit of a PrB (**46**) in methanol furnishing a 8^1,8^2-*seco*-phyllobilin

- The absorption spectra of DPxBs **64–67** feature two major peaks (~ 215 and ~ 430 nm), and the longest wavelength peaks (~ 430 nm) of *E* isomers are bathochromically shifted by ~ 8 nm compared to that of *Z* isomers (▶ **Fig. 7**, panel 7).
- The absorption spectrum of PrB **46** exhibits two major peaks (~ 315 and ~ 520 nm), as does that of DPrB **68**; the only difference is that the intensity of the first band (~ 315 nm) in DPrB **68** is hypsochromically shifted by half compared to that of PrB **46** (▶ **Fig. 7**, panel 4 and 8).
- The absorption maxima of PrB metal complexes **47–51** are bathochromically shifted by 90 ~ 120 nm compared to that of parent PrB **46** (▶ **Fig. 7**, panel 4). In a similar manner, the absorption maximum of DPrB zinc complex **69** is bathochromically shifted by ~ 100 nm compared to that of parent DPrB **68** (▶ **Fig. 7**, panel 8).

One representative phyllobilin from each category was chosen for the display of the corresponding absorption spectrum. The collected absorption spectra of the representative phyllobilins are shown in ▶ **Fig. 8**. Two major factors govern the absorption spectral properties of phyllobilins. One factor is the composition of ring A: type-I phyllobilins possess a formylpyrrole, whereas type-II phyllobilins bear a pyrrolinone. The absorption spectra of formylpyrroles and pyrrolinones are distinct: for example, 3,4,5-trimethyl-3-pyrrolin-2-one has an absorption maximum at 211 nm (ε = 14,980 $M^{-1}cm^{-1}$, in ethanol) [59], whereas 2-formyl-3,4,5-trimethylpyrrole shows an absorption maximum at 319 nm (ε = 19 500 $M^{-1}cm^{-1}$, in chloroform) (▶ **Fig. 9**) [60]. As a result, the absorption spectra of type-II phyllobilins lack the absorption bands ~ 320 nm characteristic of the formylpyrrole moiety of type-I phyllobilins (▶ **Fig. 8**).

The second factor is the saturation level of phyllobilins, which ranges from 2 (PleBs and DPleBs) to 1 (PluBs, DPluBs, PxBs, and DPxBs) to 0 (PrB and DPrB). The greater the saturation level, the shorter the path of π conjugation, and, in general, the shorter the wavelength of absorption. Although the saturation level of PluBs (DPluBs) and PxBs (DPxBs) equals 1, the absorption maxima of PxBs (DPxBs) are bathochromically shifted by > 65 nm compared to that of PluBs (DPluBs). Such a significant difference between PluBs (DPluBs) and PxBs (DPxBs) arises from the nature of the core chromophore. The structural framework of PluBs (DPluBs) consists of a formylpyrrole **A1** and a dihydrodipyrrin **B1**, while that for PxBs (DPxBs) consists of a dipyrrinone **C1** (▶ **Fig. 10**).

The analysis of the core chromophoric framework of phyllobilins is displayed in ▶ **Fig. 10**. The absorption spectra of the core chromophores and phyllobilins are compared in ▶ **Fig. 11**. The absorption spectral trace of 2-formyl-3,4,5-trimethylpyrrole (**A1**) (λ_{max} = 319 nm) [60] is not available, thus the spectral trace of 2-formylpyrrole (λ_{max} = 289 nm, in methanol) [52, 61], which is bathochromically shifted by 30 nm, was used as a surrogate of **A1**. The solvents and literature citations for the spectral traces are as follows: dihydrodipyrrin **B1** (diethyl ether) [62], dipyrrinone **C1** (dimethyl sulfoxide) [63], tripyrrinone **D1** (chloroform) [64], and zinc tripyrrinone **D2** (methanol) [65].

The absorption spectrum of RCC **1** resembles that of tripyrrinone **D1**, with slight differences of the peak shapes in the region > 450 nm, which most likely is due to the reduction of ring C from a pyrrole to a pyrroline (▶ **Fig. 11**, panel 1). The two major peaks of PluB **7** (318 and 360 nm) are ascribed to the absorptions characteristic of formylpyrrole **A1** and dihydrodipyrrin **B1** (▶ **Fig. 11**, panel 2). Note that the 30 nm gap between PluB **7** and dihydrodipyrrin **B1** can be attributed to the presence of the carbonyl group

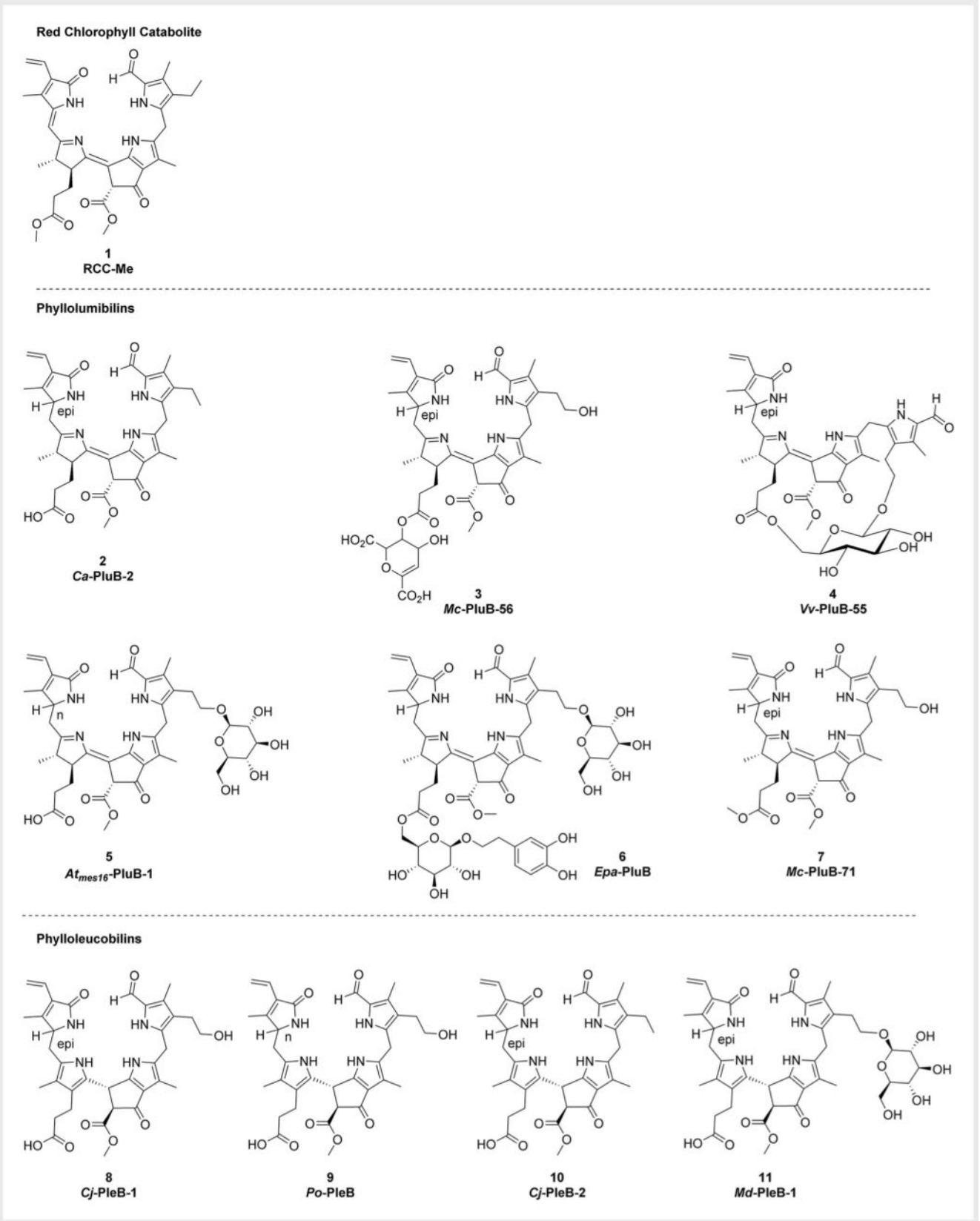

▶ **Fig. 6** Structures of phyllobilins in the database. *continued*

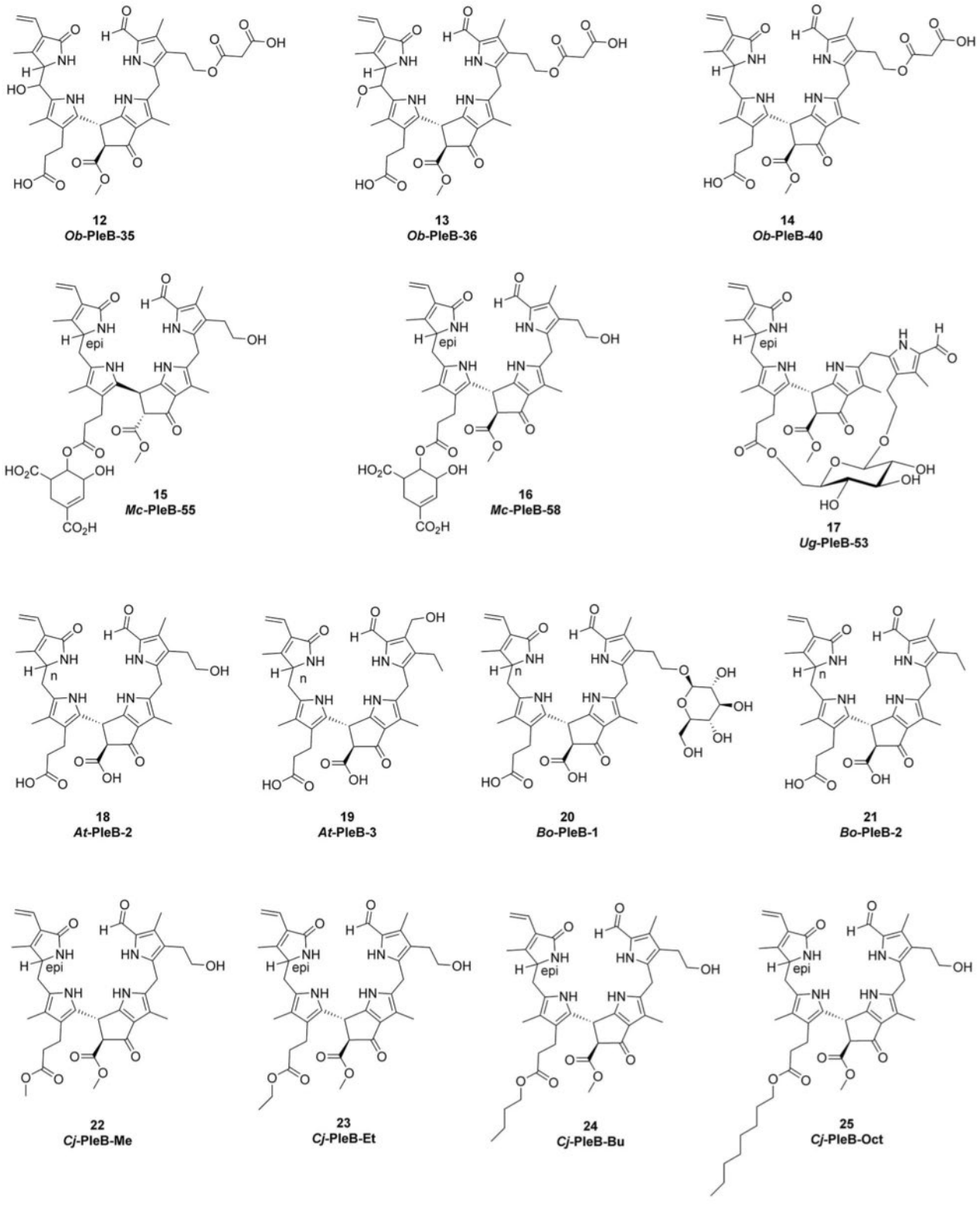

▶ **Fig. 6** *Continued*

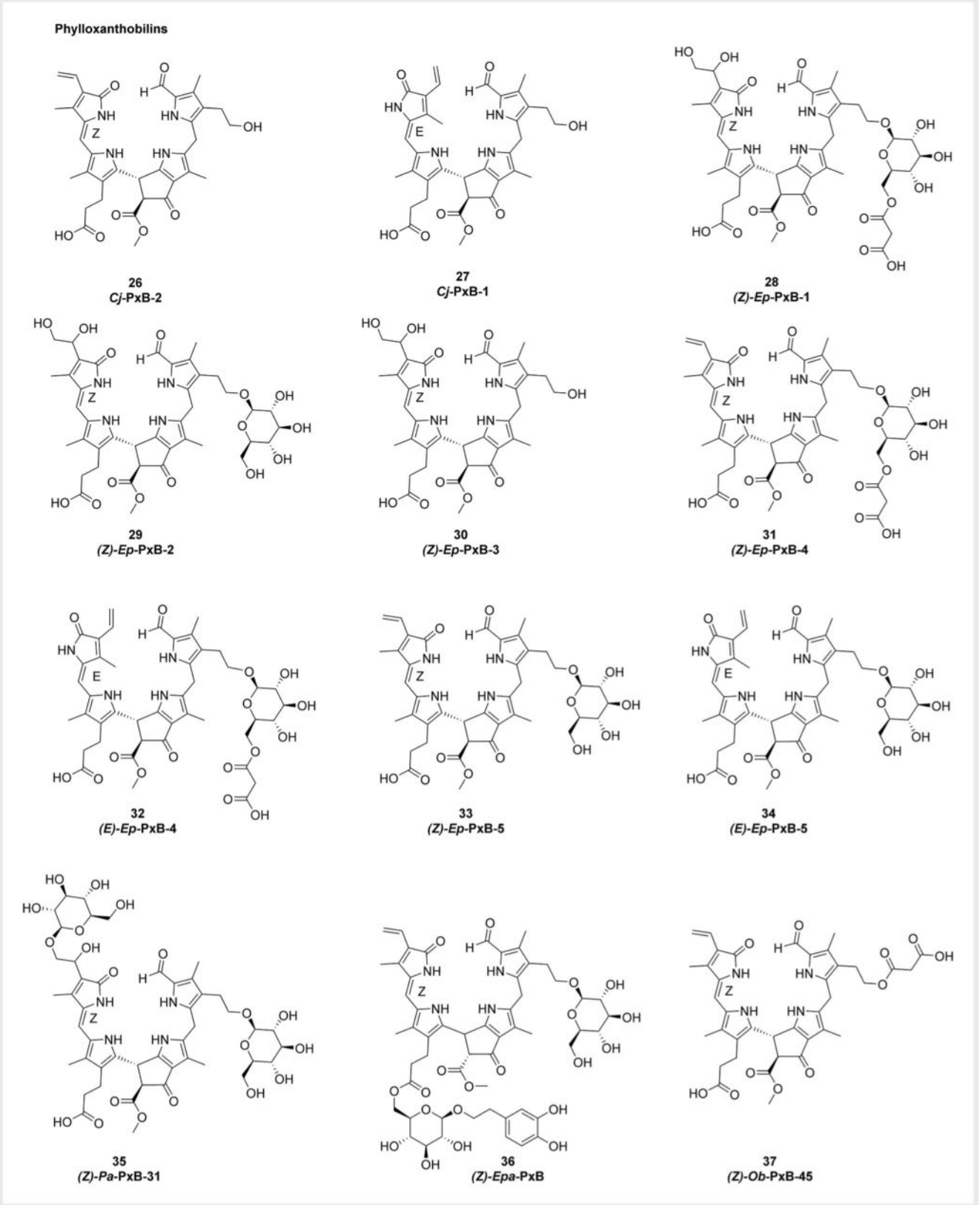

▶ **Fig. 6** *Continued*

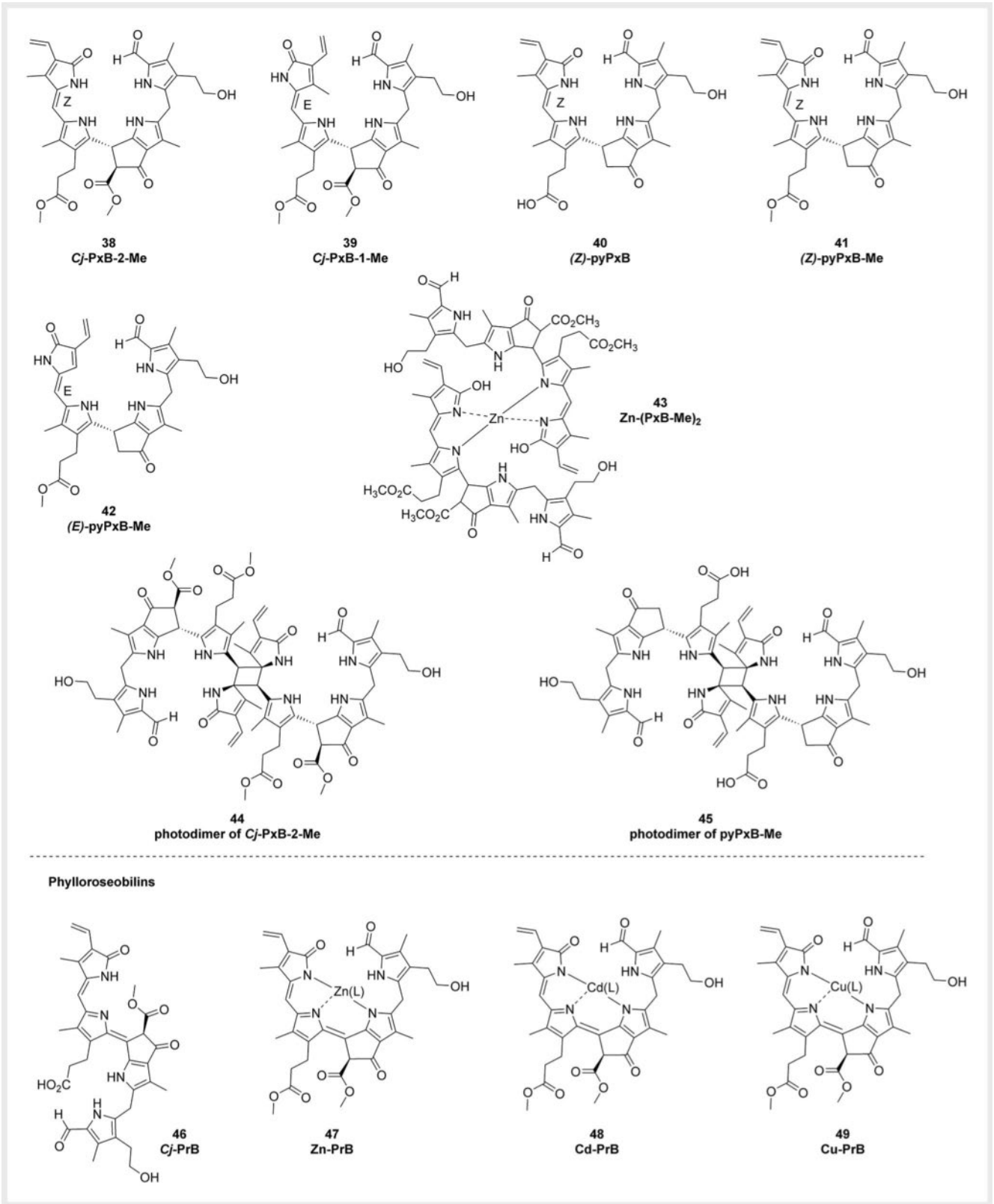

▶ **Fig. 6** *Continued*

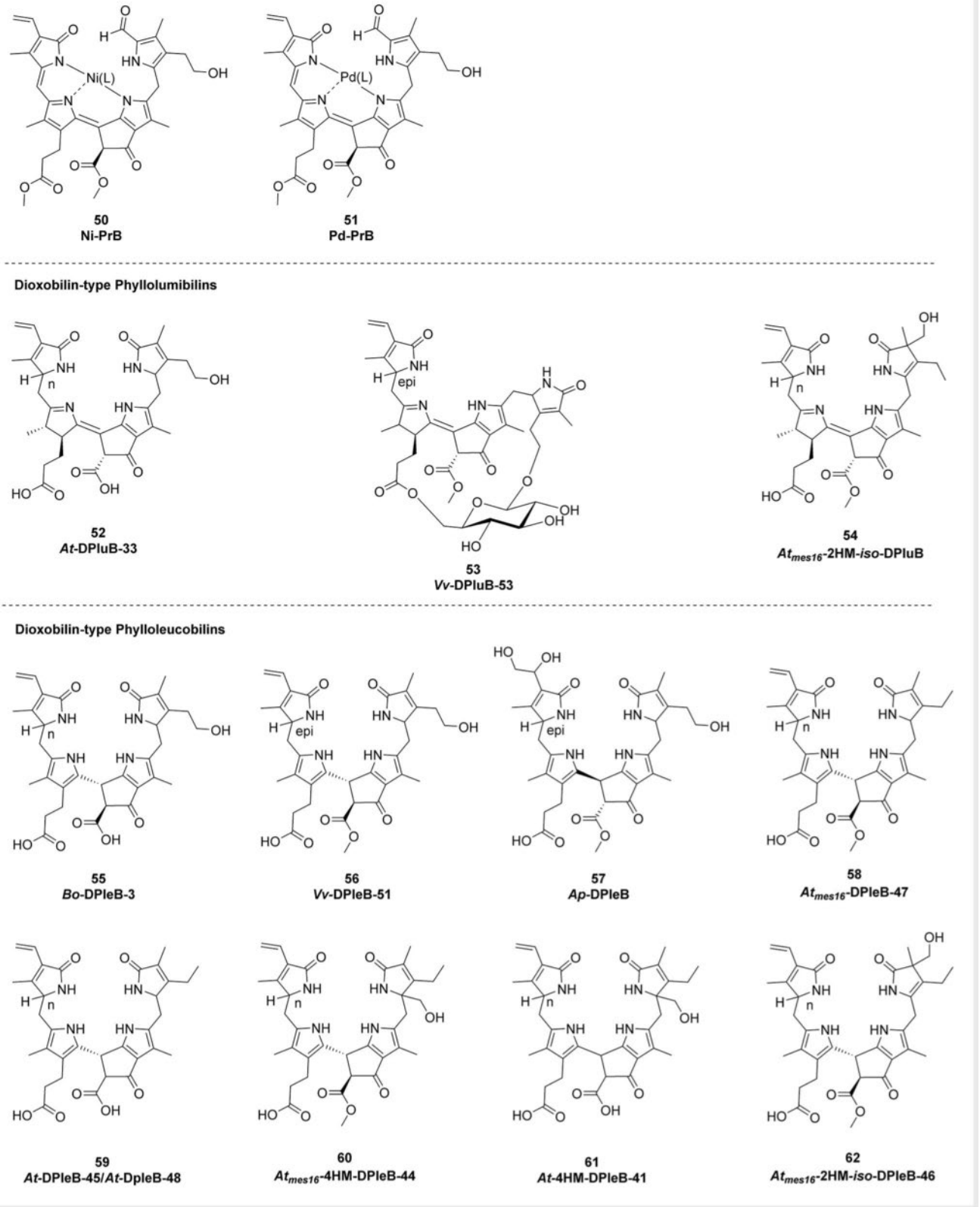

▶ **Fig. 6** *Continued*

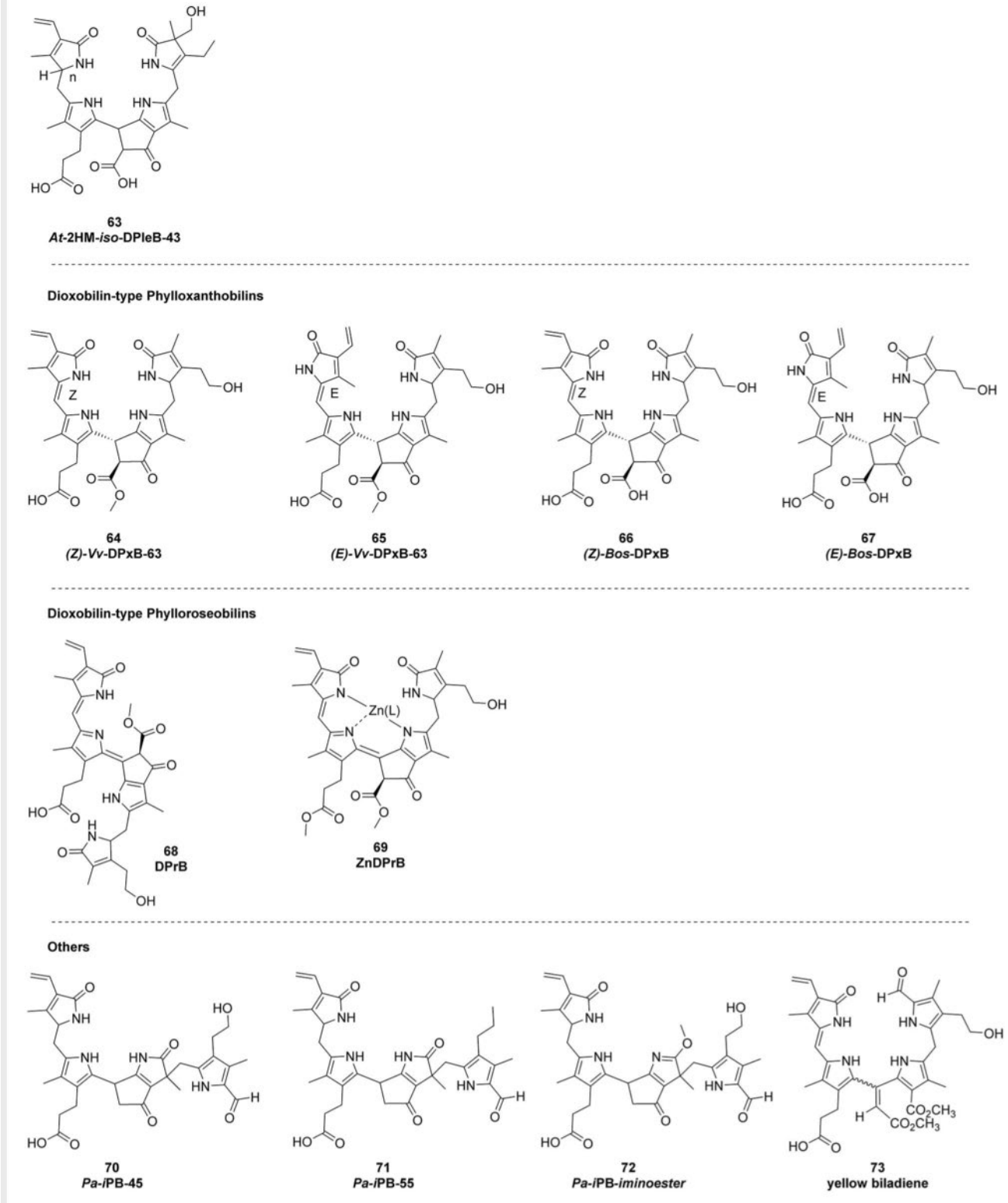

▶ **Fig. 6** *Continued*

of ring E in PluB **7**. The absorption spectrum of PleB **8** is analogous to that of formylpyrrole **A1** (▶ **Fig. 11**, panel 3). The absorption spectrum of PxB **26** is given by the sum of two chromophores, formylpyrrole **A1** and dipyrrinone **C1** (▶ **Fig. 11**, panel 4). The two absorption bands of PrB **46** (~ 315 and ~ 520 nm) match well to that of tripyrrinone **D1** except for the divergence of peak intensities

▶ **Table 2** Absorption and fluorescence spectral properties of phyllobilins.

#	Name	Solvent	Absorption maxima in nm (relative intensity)	Absorption coefficient	Fluorescence maxima in nm (quantum yield)	Reference
1	RCC-Me	EtOH	212 (0.94), 317 (1), 535 (0.33)		687 (0.036)	[24]
Phyllolumibilins (PluBs)						
2	*Ca*-PluB-2	aq. MeOH[a]	322 (1), 360 (0.70)			[55]
3	*Mc*-PluB-56	aq. MeOH[b]	235 (1), 317 (0.77), 356 (0.49)	19500 (317 nm)	447	[13]
4	*Vv*-PluB-55	MeOH	314 (1), 357 (0.74)		440	[26]
5	At_{mes16}-PluB-1	HPLC[c]	318 (1), 362 (0.73)			[42]
6	*Epa*-PluB	HPLC[d]	317 (1), 362 (0.65)			[28]
7	*Mc*-PluB-71	EtOH	318 (1), 360 (0.71)		438 (0.21)	[56]
Phylloleucobilins (PleBs)						
8	*Cj*-PleB-1	MeOH	214 (1), 241 (sh, 0.69), 314 (0.62)			[32]
		HPLC[e]	219 (1), 243 (sh, 0.77), 313 (0.68)			this publication
9	*Po*-PleB	HPLC[e]	216 (1), 243 (sh, 0.70), 314 (0.61)			this publication
10	*Cj*-PleB-2	aq. MeOH[a]	225 (1), 246 (sh, 0.76), 314 (0.69)			[55]
11	*Md*-PleB-1	MeOH	216 (1), 243 (0.73), 314 (0.69)			[32]
12	*Ob*-PleB-35	HPLC[d]	213 (1), 243 (sh, 0.73), 315 (0.66)			[33]
13	*Ob*-PleB-36	HPLC[d]	215 (1), 246 (sh, 0.60), 312 (0.88)			[33]
14	*Ob*-PleB-40	HPLC[d]	213 (1), 243 (sh, 0.67), 313 (0.62)			[33]
15	*Mc*-PleB-55	aq. MeOH[a]	211 (1), 243 (sh, 0.70), 314 (0.52)			[29]
16	*Mc*-PleB-58	aq. MeOH[a]	212 (1), 243 (sh, 0.71), 314 (0.57)			[29]
17	*Ug*-PleB-53	MeOH	218 (1), 242 (sh, 0.76), 312 (0.65)	21400 (312 nm)		[34]
18	*At*-PleB-2	unspecified	219 (1), 244 (sh, 0.67), 319 (0.52)			[57]
19	*At*-PleB-3	unspecified	219 (1), 243 (sh, 0.69), 324 (0.64)			[57]
20	*Bo*-PleB-1	HPLC[d]	214 (1), 244 (sh, 0.66), 315 (0.62)			[37]
21	*Bo*-PleB-2	HPLC[d]	215 (1), 242 (sh, 0.66), 318 (0.51)			[37]
22	*Cj*-PleB-Me	HPLC[e]	220 (1), 241 (sh, 0.84), 311 (0.70)			this publication
23	*Cj*-PleB-Et	HPLC[e]	222 (1), 243 (sh, 0.87), 311 (0.73)			this publication
24	*Cj*-PleB-Bu	HPLC[e]	228 (1), 310 (0.78)			this publication
25	*Cj*-PleB-Oct	HPLC[e]	232 (1), 308 (0.74)			this publication
Phylloxanthobilins (PxBs)						
26	*Cj*-PxB-2	HPLC[e]	220 (0.60), 246 (0.52), 312 (0.67), 426 (1)			this publication
27	*Cj*-PxB-1	HPLC[e]	218 (0.93), 248 (0.74), 312 (1), 438 (0.92)			this publication
28	(*Z*)-*Ep*-PxB-1	HPLC[e]	212 (1), 242 (sh, 0.81), 314 (0.65), 410 (0.51)			[8]
29	(*Z*)-*Ep*-PxB-2	HPLC[e]	208 (1), 242 (0.75), 314 (0.76), 414 (1)			[8]
30	(*Z*)-*Ep*-PxB-3	HPLC[e]	208 (0.94), 242 (0.73), 314 (0.82), 414 (1)			[8]
31	(*Z*)-*Ep*-PxB-4	HPLC[e]	216 (0.80), 246 (0.58), 314 (0.72), 426 (1)			[8]
32	(*E*)-*Ep*-PxB-4	HPLC[e]	214 (1), 248 (0.66), 312 (0.84), 436 (0.65)			this publication
33	(*Z*)-*Ep*-PxB-5	HPLC[e]	216 (0.79), 246 (0.55), 312 (0.71), 426 (1)			[8]
34	(*E*)-*Ep*-PxB-5	HPLC[e]	216 (1), 248 (0.71), 312 (0.96), 438 (0.8.)			this publication

continued

▶ **Table 2** *Continued*

#	Name	Solvent	Absorption maxima in nm (relative intensity)	Absorption coefficient	Fluorescence maxima in nm (quantum yield)	Reference
35	(*Z*)-*Pa*-PxB-31	HPLC[d]	246 (0.66), 314 (0.99), 418 (1)			[21]
36	(*Z*)-*Epa*-PxB	HPLC[d]	276 (0.86), 313 (1), 423 (0.4)			[28]
37	(*Z*)-*Ob*-PxB-45	HPLC[d]	214 (sh, 1), 246 (0.58), 315 (0.65), 426 (0.77)			[33]
38	*Cj*-PxB-2-Me	MeOH	311 (0.69), 422 (1)		485	[38,40]
		EtOH	311 (0.64), 425 (1)		488	[38,40]
		$CHCl_3$	322 (0.68), 422 (1)		648	[38,40]
		toluene	328 (0.99), 426 (1)		665	[38,40]
		DMSO	308 (0.86), 430 (1)	39800 (430 nm)	493	[58]
39	*Cj*-PxB-1-Me	MeOH	310 (1), 429 (0.82)	22900 (310 nm)	489	[38]
40	(*Z*)-pyPxB	MeOH	310 (0.73), 427 (1)			[39]
41	(*Z*)-pyPxB-Me	MeOH	310 (0.58), 426 (1)	42700 (426 nm)		[39]
		$CHCl_3$	319 (0.60), 424 (1)	40700 (424 nm)		[39]
42	(*E*)-pyPxB-Me	MeOH	310 (1), 433 (0.82)	22900 (310 nm)		[39]
		$CHCl_3$	313 (1), 424 (0.84)	21400 (313 nm)		[39]
43	Zn-$(PxB\text{-}Me)_2$	DMSO	319 (0.72), 484 (1)		538	[58]
44	photodimer of *Cj*-PxB-2-Me	$CHCl_3$	270 (sh, 0.89), 323 (1)	40700 (323 nm)		[38]
45	photodimer of pyPxB-Me	$CHCl_3$	268 (sh, 0.93), 323 (1)	38900 (323 nm)		[39]
Phylloroseobilins (PrBs)						
46	*Cj*-PrB	MeOH	313 (0.72), 523 (1)	36300 (523 nm)	621	[19]
		HPLC[e]	230 (0.35), 309 (0.68), 524 (1)			this publication
47	Zn-PrB	MeOH	318 (0.84), 620 (1)	26900 (620 nm)	650	[19]
48	Cd-PrB	MeOH	317 (0.64), 613 (1)	33100 (613 nm)	647	[19]
49	Cu-PrB	MeOH	323 (0.89), 635 (1)	24000 (635 nm)		[19]
50	Ni-PrB	MeOH	326 (0.67), 626 (1)	25700 (626 nm)		[19]
51	Pd-PrB	MeOH	332 (0.99), 645 (1)			[40]
Dioxobilin-type Phyllolumibilins (DPluBs)						
52	*At*-DPluB-33	HPLC[d]	217 (1), 247 (sh, 0.61), 361 (0.48)			[41]
53	*Vv*-DPluB-53	MeOH	357		435	[26]
54	At_{mes16}-2HM-*iso*-DPluB	MeOH	222 (1), 244 (0.95), 358 (0.73)			[42]
Dioxobilin-type Phylloleucobilins (DPleBs)						
55	*Bo*-DPleB-3	HPLC[d]	216 (1), 248 (sh, 0.54), 288 (sh, 0.19)			[41]
56	*Vv*-DPleB-51	MeOH	212 (1), 242 (sh, 0.66), 286 (sh, 0.18)	41600 (212 nm)		[26]
57	*Ap*-DPleB	MeOH	210 (1), 244 (sh, 0.49), 284 (sh, 0.16)	56200 (210 nm)		[43]
58	At_{mes16}-DPleB-47	HPLC[c]	213 (1), 243 (sh, 0.65), 284 (sh, 0.16)			[42]
59	*At*-DPleB-45/ At-DPleB-48	HPLC[d]	215 (1), 244 (sh, 0.63)			[44]

continued

▶ **Table 2** *Continued*

#	Name	Solvent	Absorption maxima in nm (relative intensity)	Absorption coefficient	Fluorescence maxima in nm (quantum yield)	Reference
60	At_{mes16}-4HM-DPleB-44	HPLC[c]	213 (1), 246 (sh, 0.59), 286 (sh, 0.15)			[42]
61	*At*-4HM-DPleB-41	HPLC[d]	215 (1), 243 (sh, 0.64)			[44]
62	At_{mes16}-2HM-*iso*-DPleB-46	HPLC[c]	215 (1), 246 (sh, 0.74)			[42]
63	*At*-2HM-*iso*-DPleB-43	HPLC[d]	216 (1), 246 (sh, 0.68)			[44]
Dioxobilin-type Phylloxanthobilins (DPxBs)						
64	(*Z*)-*Vv*-DPxB-63	HPLC[e]	216 (1), 244 (sh, 0.63), 282 (sh, 0.25), 426 (0.87)			this publication
65	(*E*)-*Vv*-DPxB-63	HPLC[e]	224 (1), 242 (0.93), 276 (0.49), 434 (0.91)			this publication
66	(*Z*)-*Bos*-DPxB	HPLC[e]	216 (1), 242 (0.64), 280 (sh, 0.26), 430 (1)			[45]
67	(*E*)-*Bos*-DPxB	HPLC[e]	214 (1), 244 (sh, 0.57), 282 (sh, 0.32), 438 (0.61)			this publication
Dioxobilin-type Phylloroseobilins (DPrBs)						
68	DPrB	MeOH	318 (0.38), 521 (1)		649	[46]
69	ZnDPrB	MeOH	357 (0.66), 619 (1)	25 100 (619 nm)	658	[46]
		CH_3CN	368 (0.99), 581 (0.98), 626 (1)	17 800 (626 nm)		[46]
Others						
70	Pa–*i*PB-45	MeOH	212 (1), 290 (0.72)			[47]
71	Pa–*i*PB-55	MeOH	214 (1), 286 (0.77), 310 (0.68)			[47]
72	Pa–*i*PB-iminoester	MeOH	216 (0.86), 274 (1), 312 (sh, 0.65)			[47]
73	yellow biladiene	aq. MeOH[a]	314 (0.94), 462 (1)			[48]

[a] Methanol and PPB, pH 7; [b] Methanol/water = 9 : 1; [c] Methanol and aqueous NH_4OAc; [d] Methanol and PPB; [e] Acetonitrile and aqueous NH_4OAc pH = 7.
sh = shoulder.

▶ **Fig. 7** Absorption spectra of phyllobilins. (1) PluBs, (2) PleBs, (3) PxBs, (4) PrBs and their metal complexes; all type-I phyllobilins at the left panel. (5) DPluBs, (6) DPleBs, (7) DPxBs, (8) DPrB and its metal complex; all type-II phyllobilins at the right panel.

(▶ **Fig. 11**, panel 5). The absorption maxima of PrB zinc complex **47** (620 nm) appears similar in position to that of zinc tripyrrinone **D2** (610 nm), albeit accompanied by broadening to nearly double the peak width (▶ **Fig. 11**, panel 6).

Structural Modifications and Diversity of Phyllobilins

We now provide an overview of the structural modifications of phyllobilins that underlie the diversity illustrated in ▶ **Table 1** and **Fig. 1**. The presentation reports the knowledge available concerning enzymatic or non-enzymatic pathways that give rise to structural diversity. The key resulting spectral features are reported in this context for representative phyllobilins.

RCC – a progenitor of all phyllobilins. The red chlorophyll catabolite is the product of an early step of the chlorophyll degradation pathway, the oxygenolytic opening of the chlorophyll macrocycle by PAO. The resulting linear 1-formyl-oxo phyllobilin is the precursor of all downstream phyllobilins [66]. The RCC remained, however, a 'cryptic' component of chlorophyll breakdown, until the methyl ester, RCC-Me (**1**), could be generated by partial synthesis from the methyl ester of pheophytin *a* (the free base analogue of chlorophyll *a*) [67]. Interestingly, blockage of the biochemical program at the stage of the RCC by the absence of RCCR results in a light-dependent cell death, assumed to be caused by photo-

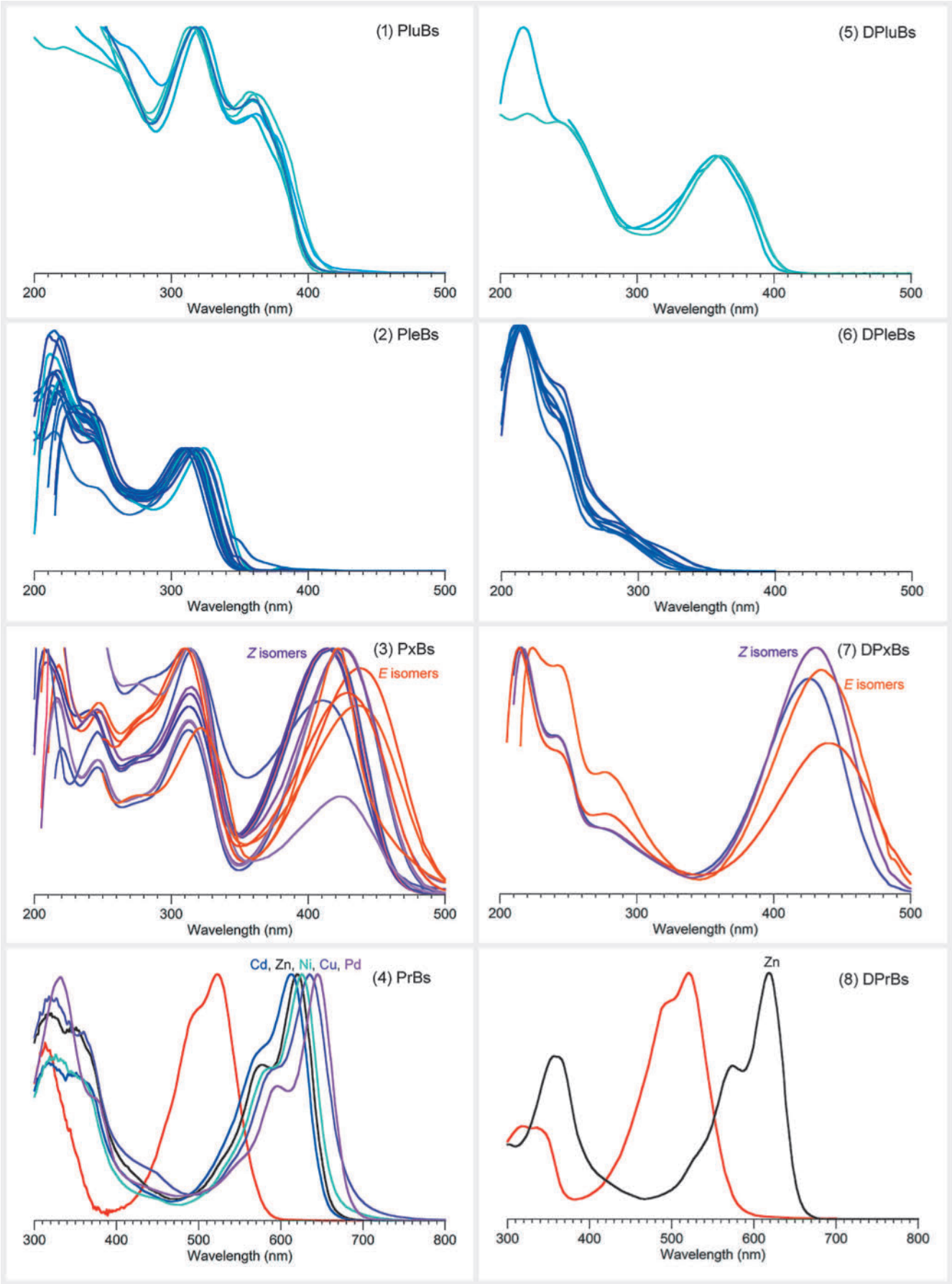
(1) PluBs
200
300
400
500
Wavelength (nm)
(5) DPluBs
200
300
400
500
Wavelength (nm)
(2) PleBs
200
300
400
500
Wavelength (nm)
(6) DPleBs
200
300
400
500
Wavelength (nm)
Z isomers
E isomers
(3) PxBs
200
300
400
500
Wavelength (nm)
Z isomers
E isomers
(7) DPxBs
200
300
400
500
Wavelength (nm)
Cd, Zn, Ni, Cu, Pd
(4) PrBs
300
400
500
600
700
800
Wavelength (nm)
Zn
(8) DPrBs
300
400
500
600
700
800
Wavelength (nm)

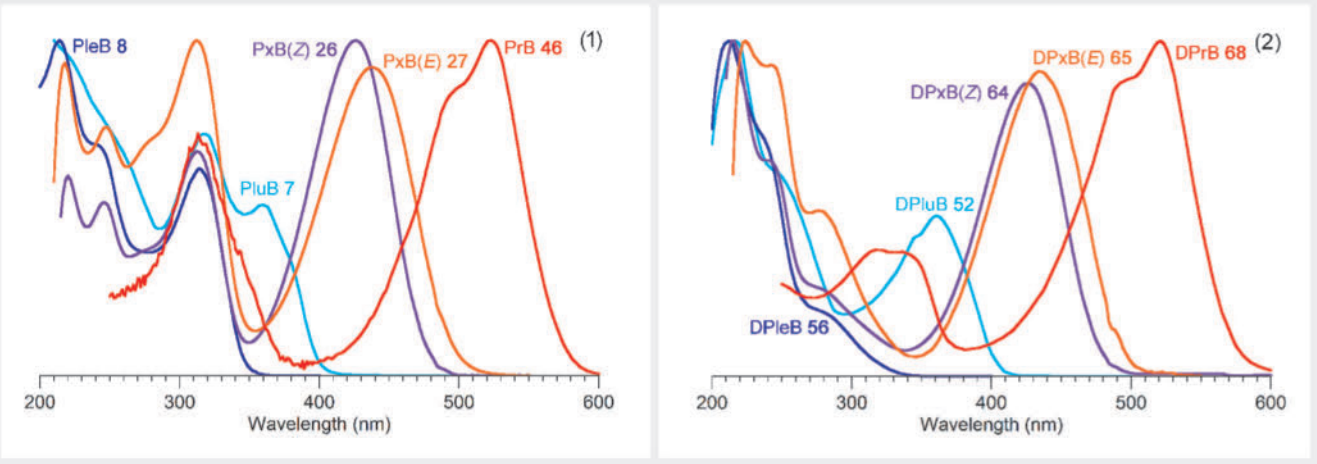

▶ **Fig. 8** Absorption spectra of selected phyllobilins (one from each category). (1) PluB **7**, PleB **8**, PxB(*Z*) **26**, PxB(*E*) **27**, and PrB **46**. (2) DPluB **52**, DPleB **56**, DPxB(*Z*) **64**, DPxB(*E*) **65**, and DPrB **68**.

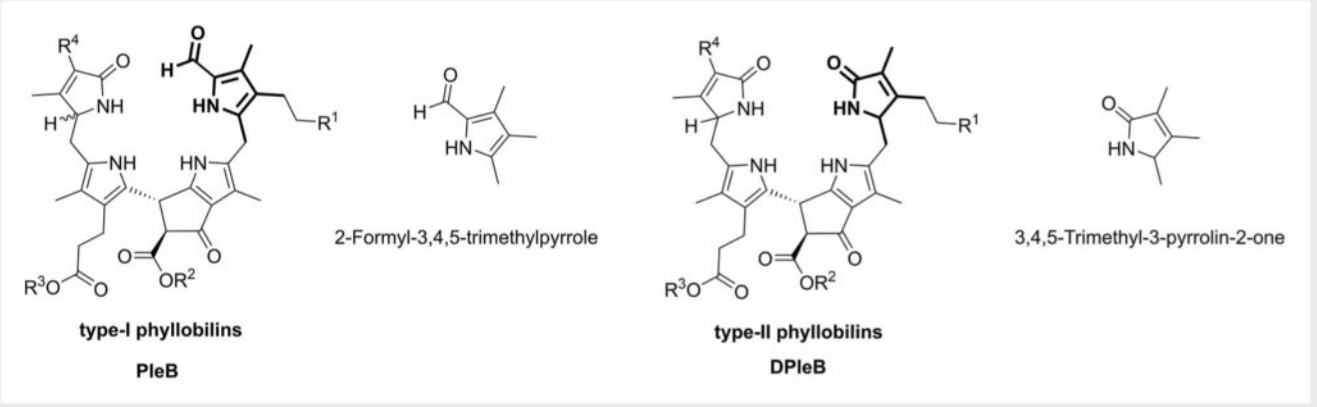

▶ **Fig. 9** The distinctive structural backbone of type-I and type-II phyllobilins in ring A.

chemical properties of the arrested RCC and pheophytin *a* intermediates [68]. Nevertheless, **1** proved to be an inefficient sensitizer of singlet oxygen, indicating the lethality must stem from non-photodynamic molecular mechanisms that trigger cell death in plant mutants lacking RCCR [24]. The characteristic and eponymous color of RCC stems from the absorption at 535 nm, as shown for RCC-Me (**1**) (▶ **Fig. 11**, panel 1).

Structural modifications at ring A. The composition of ring A defines a type-I or type-II phyllobilin because of the presence of a formylpyrrole or pyrromethanone, respectively. Most of the phyllobilins, regardless of type, are modified at the 3^2 carbon by a 'simple' hydroxyl group. The hydroxylation is attributed to a Rieske-type oxygenase, called 'translocon at the inner chloroplast envelope' (TIC55) [69]. For *p*PluB (**2**), for example, the resulting 3^2-OH PluB is exported to the cytosol, where further modification reactions take place, such as glycosylation (e.g., **11**) or malonylation (e.g., **12**), depending on the plant species [23]. In many plants, however, the unmodified 3^2-OH PluB was found to be the predecessor of PleBs, and the 3^2-OH-PleB is still the most commonly identified phyllobilin structure, isolated from leaves of *Cercidiphyllum japonicum* (**8**), apple, and spinach, among others [30, 32, 70]. Such modifications of the 3^2-OH (or even formation of the 3^2-OH) group cause hardly any change in the spectral properties (▶ **Fig. 7**, panel 2), which is not surprising given the distance from the π-chromophore.

The plant *Arabidopsis thaliana* was the first model organism established as a molecular and post-genomic tool to identify and study plant proteins [71], and it has also enabled the identification of a variety of enzymes involved in the chlorophyll degradation pathway [23]. A large number of different phyllobilin structures have been elucidated in *A. thaliana*, of which more than 90% appear to be type-II dioxobilin-type phyllobilins [42, 72]. In addition to identified PleBs and DPleBs featuring rather common modification motifs, structures with puzzling exceptional modifications have also been discovered. Structural elucidation of one PleB fraction revealed a hydroxymethyl group at C2 instead of a methyl unit, which has been assumed to be derived from chlorophyll *b* because of insufficient reduction of the C2 formyl group (**19**) [36]. As stated earlier, ordinarily, chlorophyll *b* is reduced to chlorophyll *a*, and the latter is then funneled into the catabolic path-

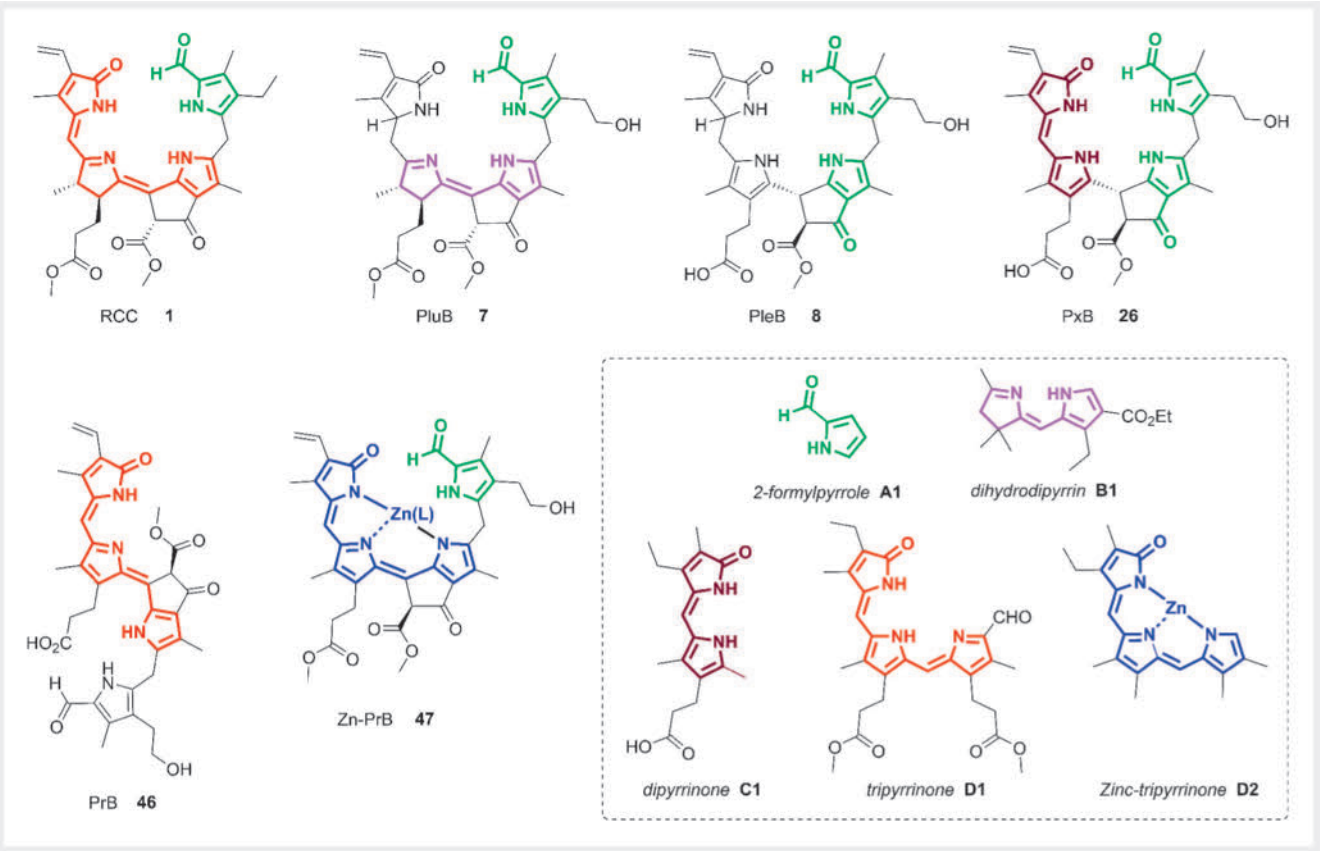

▶ **Fig. 10** The core chromophoric framework of phyllobilins.

way, yielding phyllobilins. Further phyllobilins were identified in wild type *A. thaliana*, as well as in the Mes16-mutant (see below), which stand out because of a carbon-hydroxymethylation either at the C2 (**62** and **63**) or at C4 (**60** and **61**) [42,44]. In each case, a π-interrupting quaternary carbon is formed. The absorption spectra of **60–63** are quite similar to each other (▶ **Fig. 7**, panel 6).

Structural modifications at ring B/E. One major structural difference between phyllobilins and the heme-derived bilins is the chlorophyll-characteristic additional cyclopentanone unit featuring a methoxycarbonyl moiety at the southern hemisphere of the phyllobilin molecule (▶ **Fig. 5**) [73]. Many phyllobilins from different plant species (e.g., from broccoli **20** and **21** [37]), however, carry a free acid functionality resembling the diacid structure of the bilins. Mes16, a methyl esterase, was found to be responsible for the demethylation of the carboxymethyl group at $C8^2$ at the stage of the PluB in *Arabidopsis thaliana* (**5**), which leads to the accumulation of phylloleucobilins lacking the methyl ester (**18** and **19**). Accordingly, only phyllobilins equipped with a methyl ester were observed in a Mes16 mutant of *A. thaliana* (At_{mes16}-phyllobilins, e.g., **58**) [27]. Compound **58** lacks the formylpyrrole chromophore and consequently lacks the peak at ~ 320 nm observed for the absorption spectra of **18–21**, which do contain the formylpyrrole unit (▶ **Fig. 9**).

Surprisingly, the free carboxy group at ring E of phyllobilins was found to be quite stable and resistant against the loss of carbon dioxide, even though part of a β-ketoacid; phyllobilins lacking the carboxy unit, however, so called pyro-phyllobilins (**41** and **42**), could be generated by decarboxylation under harsh synthetic conditions [39]. Even though such synthetically produced pyro-phyllobilins have not yet been identified in nature, in bracken fern, phyllobilin structures have indeed been discovered that resemble pyro-phyllobilins because of the lack of a carboxyl unit, but additionally exhibit an exceptional rearranged carbon skeleton at ring A (**70, 71** and **72**). These so-called iso-phyllobilins were the first chlorophyll catabolites isolated from a seedless vascular plant, and the exceptional structure indicated clear differences in the chlorophyll breakdown process between angiosperms and gymnosperms [47]. Such distinctions point to evolutionary differences in chlorophyll catabolism, the ramifications of which are not yet understood. The core chromophore of iso-phyllobilins **70–72** is a 2-formyl pyrrole. Consequently, their absorption spectra are similar to that of 2-formyl-3,4,5-trimethylpyrrole (**A1**), which exhibits absorption maxima at 275 and 319 nm (▶ **Fig. 9**) [60].

Structural modifications at ring C. Synthetic modification of the propionic acid side chain at C12 of the PluB to form a methyl ester derivative imparted increased stability and was found to alter the kinetics of the transition to PleBs [14]. Analogous persistent PluBs were also discovered in nature, e.g., in ripe banana peels, giving a mesmerizing blue luminescence of bananas under black light illumination (**3** and **7**) [13]. The main *hm*PluB from banana peels turned out to be esterified by a daucic acid group (**3**); two minor PleB-daucyl esters from banana (**15** and **16**, C10 isomers) were

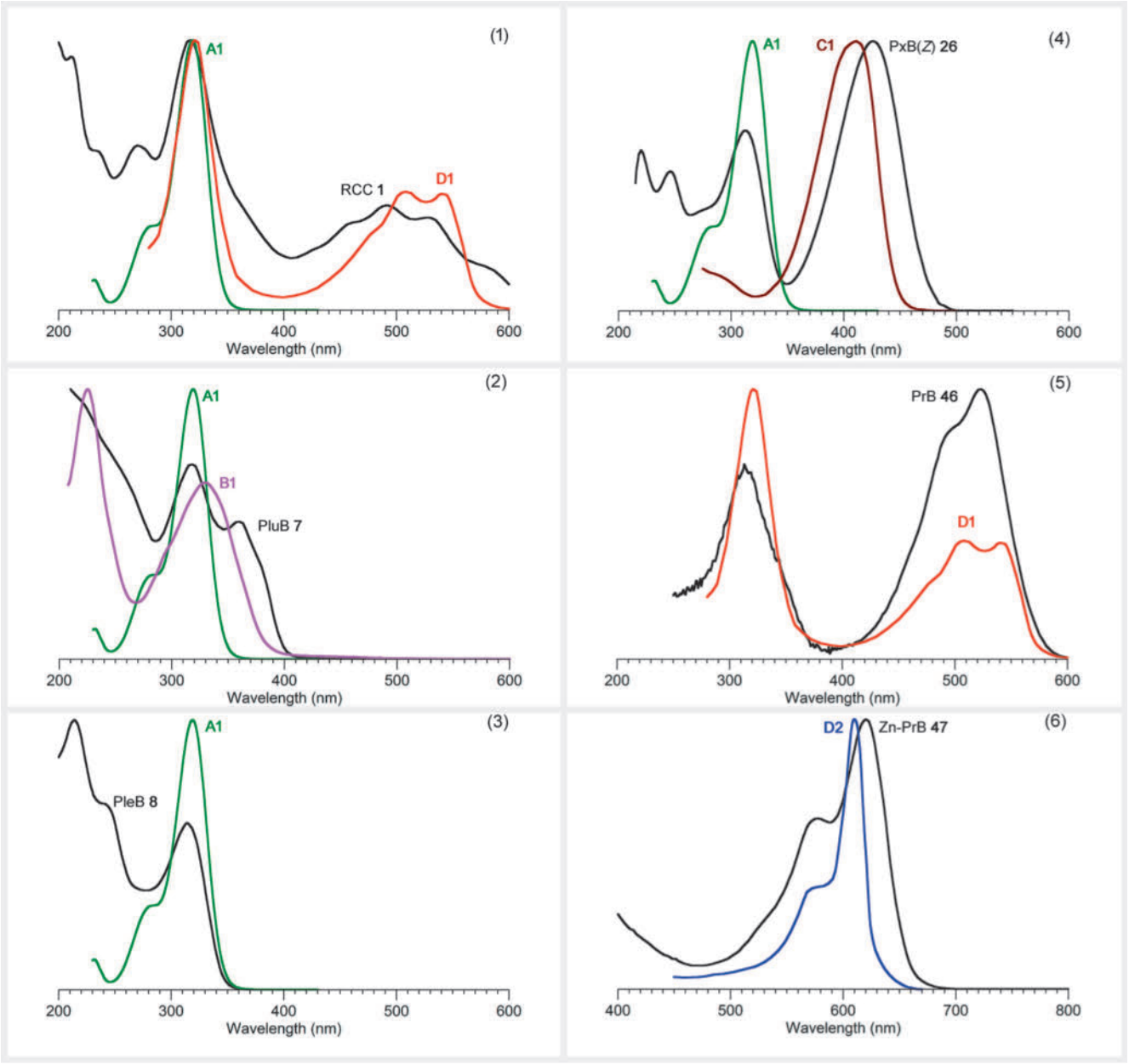

▶ **Fig. 11** Absorption spectra of (1) RCC **1**, formylpyrrole **A1**, and tripyrrinone **D1**, (2) PluB **7**, formylpyrrole **A1**, and dihydrodipyrrin **B1**, (3) PleB **8** and formylpyrrole **A1** (4) PxB **26**, formylpyrrole **A1**, and dipyrrinone **C1**, (5) PrB **46** and tripyrrinone **D1**, and (6) Zn-PrB **47** and tripyrrinone **D2**.

tentatively identified as the products of isomerization of **3** [29]. An esterified propionic acid side chain was also identified in PluB and PxB catabolites isolated from *Epipremnun aureum* (**6** and **36**) [28]. Similar but remarkable PluB, DPluB, and PleB catabolites were found in leaves of wych elm and grapevine (**4, 17** and **53**) [26, 34]. Here, the esterification links the propionic side chain to the 3^2-OH, resulting in macrolides. The macrolide architecture barely affects the absorption spectra, which are similar to those of the corresponding parent compounds.

Modification of the propionic acid side chain is not only of high relevance for the stability of phyllobilins, but also for pharmacological activities. Chemical esterification of the PleB from *Cercidiphyllum japonicum* to *Cj*-PleB-esters with alkyl residues of different chain lengths (**22–25**) led to an enhanced uptake of the phyllobilins in cancer cells, as well as an increase in anti-proliferative activity depending on the chain length. Un-esterified PleB showed no anti-proliferative effect [31]. The results to date, while limited, suggest as-yet unexplored possible therapeutic thrusts on the basis of phyllobilin scaffolds.

Structural modifications at ring D. The different structural variants at the northwestern hemisphere of the phyllobilin structure identified to date have chiefly been a vinyl moiety and a dihydroxyethyl group. One further variant is a glycosylated dihydroxyethyl group in a PleB from senescent leaves of plum trees and a PxB from senescent leaves of apricot trees (**35**) [21, 74]. Although no significant differences in ultraviolet absorption prop-

erties are observed among PleBs, the conversion of the vinyl group to a dihydroxyethyl group attached to PxBs causes a hypsochromic shift of the absorption maximum from ~ 426 nm to ~ 416 nm [8].

Phyllochromobilins – late-stage phyllobilin pigments. The discovery of the first colorless degradation product of chlorophyll, a phylloleucobilin, occurred in 1991 [73], and PleBs and DPleBs were long assumed to represent the 'final' breakdown products of the chlorophyll detoxification process. It took more than a decade for this hypothesis to be disproven and for the first yellow pigment derived from chlorophyll breakdown (**26**) [16] to be discovered. Though the exact mechanism and the enzyme(s) involved are still unclear, PleBs and their C16 isomers are transformed by an endogenous oxidation process to polar PleB intermediates that carry either a hydroxyl group or a methoxy group at C15 depending on the solvent. These polar precursors are converted to the same (*Z*)-PxB in the lab by acid-induced elimination of water or methanol, respectively [17], but in the case of the hydroxylated compound, could also be detected naturally, e.g., in senescent leaves of basil (**12** and **13**) as inferred precursors of the PxB from basil leaves (**37**) [33]. Spectral effects caused by the hydroxylation are insignificant.

Beside yellow pigments, which contribute to the fall colors in senescent leaves [16], oxidation products of PxBs, the phylloroseobilins (PrBs), were also discovered to occur naturally, albeit in minor amounts, e.g., in senescent leaves of *Cercidiphyllum japonicum* [18]. PxBs and PrBs, summarized as so-called phyllochromobilins [22, 66], not only stand out because of their intensive color, but mainly because they exhibit intriguing chemical characteristics (see below).

Bioactive Properties of Phyllobilins

Numerous phyllobilins have been subjected to a host of assays for biological activities including *in vitro* as well as cellular studies concerning anti-oxidative and anti-inflammatory activities, among others. In general, phyllobilins have been proven to be stable in biological media such as cell culture media, as well as in human blood [7, 8]. A comprehensive review of the resulting bioactivities of phyllobilins has been published very recently [5]. The objective here is not to recount all studies but rather to highlight representative biological activities for selected phyllobilins in medicinal plants and the differences in potency among phyllobilin types.

Despite the rising popularity of herbal remedies and improved phytochemical profiling, the active principles of many phytotherapeutics are not completely understood. Furthermore, the bioactive ingredients identified to date often cannot account for all observed therapeutic effects. Efficacy and quality testing in those remedies is restricted to supposedly active markers, and maintaining a reliable efficacy can be cumbersome. Due to their rather late discovery and their perceived role solely as byproducts of the chlorophyll detoxification process, phyllobilins have been overlooked and omitted in phytochemical profiling of medicinal plants by the research community. Our recent studies on the presence of phyllobilins in the medicinal plants *Echinacea purpurea* and *Urtica dioica* and their contribution to the health benefits of the plant, however, emphasize the importance of including this family of tetrapyrrolic natural products in the portfolio of bioactive phytochemicals. In the example of *Echinacea*, a plant with undoubted high importance in phytotherapy, for which many different pharmacological activities have been demonstrated, neither a single compound nor a compound class has been identified that can account for all the efficacies. Phyllobilins were shown to contribute to the health-promoting effects of the medicinal plant since a high antioxidant potential of PxBs was demonstrated. The activities of *Echinacea* PxBs were even superior to the established *Echinacea* antioxidant caffeic acid in *in vitro* experiments and were comparable to caffeic acid in cellular approaches. In addition, the PxBs were able to scavenge reactive oxygen species in cells and to protect the cells from oxidative stress [8]. Furthermore, a PxB (same structure as **33**) was also found to contribute to the health benefits of the medicinal stinging nettle (*Urtica dioica*) plant. One cup of nettle tea was shown to contain significant amounts (up to 100 µg) of PxB. Again, as for *Echinacea*, the anti-oxidative potential of PxB from *Urtica* was as high as the relevant established antioxidant compounds in nettle extracts, such as rutin, caffeic acid, and chlorogenic acid, and the PxB inhibited the central pro-inflammatory enzymes COX-1, as well as COX-2, proving its anti-inflammatory effect [7].

Originally considered 'mere' leftovers of chlorophyll detoxification, phyllobilins and, in particular, phylloxanthobilins have now gained attention because of their bioactivities contributing to health-promoting effects. Since the first report of PxBs [16], an increasing number and variety of PxBs have been identified in various plant species, e.g., an unprecedented structural variety of PxBs has been demonstrated in senescent leaves of *Echinacea purpurea* [8]. Paper spray mass spectrometry showed that PxBs do not represent artifacts of an isolation procedure but do clearly occur in more plant species than previously assumed, e.g., in spinach and peace lily, for which only PleBs had been identified before [17, 70]. Although PleBs remain the best-characterized phyllobilin structures, recent research demonstrates that, with regard to bioactivities, the PxBs significantly exceed their PleB precursors. An *in vitro* and cellular approach of the anti-oxidative activity of a PleB and a PxB (**30**) isolated from the peels of aged cucumber revealed the PxB to possess up to twice the anti-oxidative activity compared to the PleB [75]. This difference in bioactivities becomes even more obvious regarding effects on cancer cells. A PleB and its C16 isomer (**8** and **9**) were shown to possess no anti-proliferative effect on different cancer cell lines in concentrations up to 100 µM, in contrast to the common oxidation product, PxB (**26**), which was shown to be a potent inhibitor of cancer cell proliferation in the low micromolar range [31]. Thus, the core of the phyllobilin structure seems to play a crucial role regarding bioactive properties.

Since only a few examples of medicinal plants have been analyzed for their phyllobilin content to date, the identification of phyllobilins in plants should be emphasized in the future. In this regard, the database assembled herein provides the basis for straightforward analysis of crude plant extracts for the occurrence of given types of phyllobilins. In this manner, phyllobilins can be identified in medicinal plants, which may thereby broaden the repertoire of active ingredients of herbal medicines.

Transcending Biology

The discovery of phyllochromobilins has enriched the diverse pool of natural products with structures possessing interesting and exceptional chemical properties. PxBs were shown to be photoswitchable compounds, depending on the molecular environment. Due to the double bond at C15/C16, PxBs usually occur as (*E*)/(*Z*)-isomers (e.g., **26** and **27**). This isomerization is reversible and inducible by daylight in more polar solvents. In apolar environments, the *Z* isomers of PxBs can dimerize by [2 + 2] cycloadditions to the corresponding photodimers (**44** and **45**) [38]. Another predictable yet relatively unexplored property of phyllobilin pigments is their ability to coordinate in multidentate complexes with physiologically relevant divalent metal ions. Thus, a PrB afforded complexes with zinc, cadmium, copper, nickel, and palladium (**47**–**51**). Interestingly, the complexation with zinc ions serves as partial synthesis of PrBs, as adding zinc ions to PxB solutions generates the Zn-PrB complex, which can be decomplexed with acidic phosphate buffer furnishing the PrB [19]. This reaction turned out to also work for type-II phyllobilins and was utilized to create the first structure of a DPrB [20]. In addition to complexation of PrB and DPrB, a PxB-methyl ester (**38**) was shown to form a complex with a zinc ion (**43**), but this resulted in a 2 : 1 complex with different spectral properties [40]. By zinc chelation, the absorption maximum is bathochromically shifted by 58 nm, ongoing from **38** (426 nm) to **43** (484 nm). The core chromophore framework of **43** is a bis(dipyrrinato)zinc complex. The absorption maximum of an analogous coordination complex, Zn(II)-(1,3,7,9-tetramethyldipyrrin)$_2$, is reported at 486 nm [76].

Very recently, a PrB in methanolic solution upon prolonged storage was found to undergo a retro-Dieckmann reaction to give a yellow biladiene featuring an opened ring E unit (**73**). The latter resembles the structure of the heme-derived bilins, in particular bilirubin [48]. The absorption maximum of **73** appears at 465 nm, while that of bilirubin is observed at 450 nm [52].

Outlook

As recently as a generation ago, the 10^{12} kg of chlorophylls produced annually on Earth were considered to "disappear without a trace" [66]. Intense research in the ensuing years has unveiled a remarkable catabolic pathway for degradation of chlorophyll *a*. The pathway has enzymatic and non-enzymatic steps and forms phyllobilins, an unprecedented class of natural products. Initially regarded as throw-away detoxification products, phyllobilins are now known to comprise a rich collection of bioactive compounds. The view of "disappearance without a trace" can now be partly understood given that the initially formed phyllobilins (PluBs, PleBs) have hardly any absorption in the visible range, a counter-intuitive phenomenon given the strong and well-known absorption in the blue and red regions by chlorophyll *a*.

A parallel can be drawn between phyllobilins and bilins given that both derive from members of the pigments of life family, chlorophyll *a* and heme, respectively, by enzymatically controlled oxygenolysis of the macrocycle. However, the parallel is only partial because heme affords a very limited number of catabolites, whereas to date more than 70 phyllobilins are known. Phyllobilins differ in extent of π-conjugation, derivatization (e.g., hydroxylation, malonylation, glucosidation) of side chains, and number of stereocenters (bilins have no stereocenters). The entire inventory of phyllobilins is not observed in all plants or even in any plant; the variety reflects diversity of catabolic variation on a core theme among different plants. Regardless, it appears that phyllobilins are ubiquitous in plants, although the repertoire varies from plant to plant.

A surprising and emergent feature of phyllobilins concerns their beneficial effects on human health. Phyllobilins have been shown to exert antioxidant and anti-inflammatory properties in healthy human cells, as well as activities against human and murine cancer cells in culture. Far more studies are required to fully understand the mechanisms of action by which phyllobilins might exert beneficial effects in humans upon a plant-based diet. A limiting conclusion at present is that phyllobilins are valuable micronutrients for humans in a plant-based diet. The role of phyllobilins in plants remains unknown.

An interesting contrast can be drawn between phyllobilins and flavonoids, given their ubiquity in plants, vegetables, and fruit. Flavonoids, an abundant class of polyphenol secondary metabolites (but not catabolites), have been extensively studied concerning distribution in various plant species, as well as their beneficial health effects. Phyllobilins may be equally if not more abundant, albeit less visibly so, in the plant world but have until recently been little studied. The limited visible absorption of many phyllobilins as well as biochemical dogma regarding the non-utility of catabolites are two factors that likely have thwarted phytochemical profiling of plants broadly and herbal medicines in particular. The studies overviewed here suggest that the era of phyllobilins as ignored and underrated may quickly close. The spectral database presented herein provides an enabling tool to facilitate the identification of phyllobilin types in crude plant extracts. An open question is whether the phyllobilins discovered to date comprise a largely complete, extant set in nature, or are only the beginning of a vast family of natural products awaiting discovery by the plant and medical sciences community.

Contributors' Statement

Conception and design of the work: C. A. Karg, M. Taniguchi, J. S. Lindsey, S. Moser; data collection: C. A. Karg, M. Taniguchi; analysis and interpretation of the data: C. A. Karg, M. Taniguchi, J. S. Lindsey, S. Moser; drafting the manuscript: C. A. Karg, M. Taniguchi, J. S. Lindsey, S. Moser; critical revision of the manuscript: C. A. Karg, M. Taniguchi, J. S. Lindsey, S. Moser.

Acknowledgements

The authors acknowledge funding from the U.S. National Science Foundation (CHE-2054497) and from the Deutsche Forschungsgemeinschaft (DFG, German Research Foundation; Project-ID 448289381).

Conflict of Interest

The authors declare that they have no conflict of interest.

References

[1] Hörtensteiner S, Kräutler B. Chlorophyll breakdown in higher plants. Biochim Biophys Acta 2011; 1807: 977–988

[2] Hendry GAF, Houghton JD, Brown SB. The degradation of chlorophyll – a biological enigma. New Phytol 1987; 107: 255–302

[3] Kräutler B, Hörtensteiner S. Chlorophyll Breakdown: Chemistry, Biochemistry, and Biology. In: Ferreira GC, Kadish KM, Smith KM, Guilard R, eds. Handbook of Porphyrin Science (Volume 28). New Jersey: World Scientific; 2014: 117–185

[4] Tanaka R, Tanaka A. Chlorophyll cycle regulates the construction and destruction of the light-harvesting complexes. Biochim Biophys Acta 2011; 1807: 968–976

[5] Wang P, Karg CA, Frey N, Frädrich J, Vollmar AM, Moser S. Phyllobilins as a challenging diverse natural product class: Exploration of pharmacological activities. Arch Pharm 2021; 354: 2100061

[6] Moser S. Chlorophyllkataboliten in der Modellpflanze *Arabidopsis thaliana* [Diploma Thesis]. University Innsbruck: Institute of Organic Chemistry; 2005

[7] Karg CA, Doppler C, Schilling C, Jakobs F, Dal Colle MCS, Frey N, Bernhard D, Vollmar AM, Moser S. A yellow chlorophyll catabolite in leaves of *Urtica dioica* L.: An overlooked phytochemical that contributes to health benefits of stinging nettle. Food Chem 2021; 359: 129906

[8] Karg CA, Wang P, Vollmar AM, Moser S. Re-opening the stage for *Echinacea* research – Characterization of phylloxanthobilins as a novel anti-oxidative compound class in *Echinacea purpurea*. Phytomedicine 2019; 60: 152969

[9] Hörtensteiner S, Vicentini F, Matile P. Chlorophyll breakdown in senescent cotyledons of rape, *Brassica napus* L.: Enzymatic cleavage of phaeophorbide a *in vitro*. New Phytol 1995; 129: 237–246

[10] Mühlecker W, Ongania KH, Kräutler B, Matile P, Hörtensteiner S. Tracking down chlorophyll breakdown in plants: Elucidation of the constitution of a "fluorescent" chlorophyll catabolite. Angew Chem Int Ed Engl 1997; 36: 401–404

[11] Pružinská A, Anders I, Aubry S, Schenk N, Tapernoux-Lüthi E, Müller T, Kräutler B, Hörtensteiner S. *In vivo* participation of red chlorophyll catabolite reductase in chlorophyll breakdown. Plant Cell 2007; 19: 369–387

[12] Christ B, Süssenbacher I, Moser S, Bichsel N, Egert A, Müller T, Kräutler B, Hörtensteiner S. Cytochrome P450 CYP89A9 is involved in the formation of major chlorophyll catabolites during leaf senescence in *Arabidopsis*. Plant Cell 2013; 25: 1868–1880

[13] Moser S, Müller T, Ebert MO, Jockusch S, Turro NJ, Kräutler B. Blue luminescence of ripening bananas. Angew Chem Int Ed Engl 2008; 47: 8954–8957

[14] Oberhuber M, Berghold J, Breuker K, Hörtensteiner S, Kraütler B. Breakdown of chlorophyll: a nonenzymatic reaction accounts for the formation of the colorless "nonfluorescent" chlorophyll catabolites. Proc Natl Acad Sci U S A 2003; 100: 6910–6915

[15] Li C, Erhart T, Liu X, Kräutler B. Yellow dioxobilin–Type tetrapyrroles from chlorophyll breakdown in higher plants–A new class of colored phyllobilins. Chem Eur J 2019; 25: 4052–4057

[16] Moser S, Ulrich M, Muller T, Krautler B. A yellow chlorophyll catabolite is a pigment of the fall colours. Photochem Photobiol Sci 2008; 7: 1577–1581

[17] Vergeiner C, Ulrich M, Li C, Liu X, Müller T, Kräutler B. Stereo- and regioselective phyllobilane oxidation in leaf homogenates of the peace lily (*Spathiphyllum wallisii*): Hypothetical endogenous path to yellow chlorophyll catabolites. Chem Eur J 2015; 21: 136–149

[18] Ulrich M, Moser S, Müller T, Kräutler B. How the colourless 'nonfluorescent' chlorophyll catabolites rust. Chem Eur J 2011; 17: 2330–2334

[19] Li C, Ulrich M, Liu X, Wurst K, Müller T, Kräutler B. Blue transition metal complexes of a natural bilin-type chlorophyll catabolite. Chem Sci 2014; 5: 3388–3395

[20] Li C, Kräutler B. A pink colored dioxobilin-type phyllobilin from breakdown of chlorophyll. Monatsh Chem 2019; 150: 813–820

[21] Mittelberger C, Yalcinkaya H, Pichler C, Gasser J, Scherzer G, Erhart T, Schumacher S, Holzner B, Janik K, Robatscher P, Müller T, Kräutler B, Oberhuber M. Pathogen-induced leaf chlorosis: Products of chlorophyll breakdown found in degreened leaves of phytoplasma-infected apple (*Malus × domestica* Borkh.) and apricot (*Prunus armeniaca* L.) trees relate to the pheophorbide a oxygenase/phyllobilin pathway. J Agric Food Chem 2017; 65: 2651–2660

[22] Kräutler B. Phyllobilins – the abundant tetrapyrrolic catabolites of the green plant pigment chlorophyll. Chem Soc Rev 2014; 43: 6227–6238

[23] Hörtensteiner S, Hauenstein M, Kräutler B. Chlorophyll Breakdown–Regulation, Biochemistry and Phyllobilins as its Products. In: Grimm B, ed. Metabolism, Structure and Function of Plant Tetrapyrroles: Introduction, Microbial and Eukaryotic Chlorophyll Synthesis and Catabolism. Advances in Botanical Research, vol. 90. London: Elsevier; 2019: 213–271

[24] Jockusch S, Kräutler B. The red chlorophyll catabolite (RCC) is an inefficient sensitizer of singlet oxygen – photochemical studies of the methyl ester of RCC. Photochem Photobiol Sci 2020; 19: 668–673

[25] Mühlecker W, Kräutler B, Moser D, Matile P, Hörtensteiner S. Breakdown of chlorophyll: A fluorescent chlorophyll catabolite from sweet pepper (*Capsicum annuum*). Helv Chim Acta 2000; 83: 278–286

[26] Erhart T, Mittelberger C, Liu X, Podewitz M, Li C, Scherzer G, Stoll G, Valls J, Robatscher P, Liedl KR. Novel types of hypermodified fluorescent phyllobilins from breakdown of chlorophyll in senescent leaves of grapevine (*Vitis vinifera*). Chem Eur J 2018; 24: 17268–17279

[27] Christ B, Schelbert S, Aubry S, Süssenbacher I, Müller T, Kräutler B, Hörtensteiner S. MES16, a member of the methylesterase protein family, specifically demethylates fluorescent chlorophyll catabolites during chlorophyll breakdown in *Arabidopsis*. Plant Physiol 2012; 158: 628–641

[28] Roca M, Pérez-Gálvez A. Profile of chlorophyll catabolites in senescent leaves of *Epipremnun aureum* includes a catabolite esterified with hydroxytyrosol 1-O-glucoside. J Nat Prod 2020; 83: 873–880

[29] Moser S, Müller T, Holzinger A, Lütz C, Kräutler B. Structures of chlorophyll catabolites in bananas (*Musa acuminata*) reveal a split path of chlorophyll breakdown in a ripening fruit. Chem Eur J 2012; 18: 10873–10885

[30] Curty C, Engel N. Detection, isolation and structure elucidation of a chlorophyll a catabolite from autumnal senescent leaves of *Cercidiphyllum japonicum*. Phytochem 1996; 42: 1531–1536

[31] Karg CA, Wang P, Kluibenschedl F, Müller T, Allmendinger L, Vollmar AM, Moser S. Phylloxanthobilins are abundant linear tetrapyrroles from chlorophyll breakdown with activities against cancer cells. Eur J Org Chem 2020; 2020: 4499–4509

[32] Müller T, Ulrich M, Ongania KH, Kräutler B. Colorless tetrapyrrolic chlorophyll catabolites found in ripening fruit are effective antioxidants. Angew Chem Int Ed Engl 2007; 46: 8699–8702

[33] Moser S, Erhart T, Neuhauser S, Kräutler B. Phyllobilins from senescence-associated chlorophyll breakdown in the leaves of Basil (*Ocimum basilicum*) show increased abundance upon herbivore attack. J Agric Food Chem 2020; 68: 7132–7142

[34] Scherl M, Müller T, Kreutz CR, Huber RG, Zass E, Liedl KR, Kräutler B. Chlorophyll catabolites in fall leaves of the wych elm tree present a novel glycosylation motif. Chem Eur J 2016; 22: 9498–9503

[35] Pružinská A, Tanner G, Aubry S, Anders I, Moser S, Müller T, Ongania KH, Kräutler B, Youn JY, Liljegren SJ. Chlorophyll breakdown in senescent *Arabidopsis* leaves. Characterization of chlorophyll catabolites and of chlorophyll catabolic enzymes involved in the degreening reaction. Plant Physiol 2005; 139: 52–63

[36] Müller T, Moser S, Ongania KH, Pruzinska A, Hörtensteiner S, Kräutler B. A divergent path of chlorophyll breakdown in the model plant *Arabidopsis thaliana*. Chembiochem 2006; 7: 40–42

[37] Roiser MH, Müller T, Kräutler B. Colorless chlorophyll catabolites in senescent florets of broccoli (*Brassica oleracea var. italica*). J Agric Food Chem 2015; 63: 1385–1392

[38] Li C, Wurst K, Jockusch S, Gruber K, Podewitz M, Liedl KR, Kräutler B. Chlorophyll-derived yellow phyllobilins of higher plants as medium-responsive chiral photoswitches. Angew Chem Int Ed Engl 2016; 55: 15760–15765

[39] Li C, Wurst K, Berghold J, Podewitz M, Liedl KR, Kräutler B. Pyro-phyllobilins: Elusive chlorophyll catabolites lacking a critical carboxylate function of the natural chlorophylls. Chem Eur J 2018; 24: 2987–2998

[40] Li C, Kräutler B. Transition metal complexes of phyllobilins – a new realm of bioinorganic chemistry. Dalton Trans 2015; 44: 10116–10127

[41] Süssenbacher I, Hörtensteiner S, Kräutler B. A dioxobilin-type fluorescent chlorophyll catabolite as a transient early intermediate of the dioxobilin-branch of chlorophyll breakdown in *Arabidopsis thaliana*. Angew Chem Int Ed Engl 2015; 54: 13777–13781

[42] Süssenbacher I, Christ B, Hoertensteiner S, Kräutler B. Hydroxymethylated phyllobilins: A puzzling new feature of the dioxobilin branch of chlorophyll breakdown. Chem Eur J 2014; 20: 87–92

[43] Müller T, Rafelsberger M, Vergeiner C, Kräutler B. A dioxobilane as product of a divergent path of chlorophyll breakdown in Norway maple. Angew Chem Int Ed Engl 2011; 50: 10724–10727

[44] Süssenbacher I, Kreutz CR, Christ B, Hörtensteiner S, Kräutler B. Hydroxymethylated dioxobilins in senescent *Arabidopsis thaliana* leaves: sign of a puzzling biosynthetic intermezzo of chlorophyll breakdown. Chem Eur J 2015; 21: 11664–11670

[45] Karg CA, Schilling CM, Allmendinger L, Moser S. Isolation, characterization, and antioxidative activity of a dioxobilin-type phylloxanthobilin from savoy cabbage. J Porphyr Phthalocyanines 2019; 23: 881–888

[46] Li C, Podewitz M, Kräutler B. A blue zinc complex of a dioxobilin-type pink chlorophyll catabolite exhibiting bright chelation-enhanced red fluorescence. Eur J Inorg Chem 2021; 2021: 1903

[47] Erhart T, Vergeiner S, Kreutz C, Kräutler B, Müller T. Chlorophyll breakdown in a fern–Discovery of phyllobilin isomers with a rearranged carbon skeleton. Angew Chem Int Ed Engl 2018; 57: 14937–14941

[48] Li C, Kräutler B. Facile retro-Dieckmann cleavage of a pink phyllobilin: New type of potential downstream steps of natural chlorophyll breakdown. Monatsh Chem 2022. doi:10.1007/s00706-022-02894-z

[49] Taniguchi M, Lindsey JS. Absorption and fluorescence spectral database of chlorophylls and analogues. Photochem Photobiol 2021; 97: 136–165

[50] Taniguchi M, Du H, Lindsey JS. PhotochemCAD 3: Diverse modules for photophysical calculations with multiple spectral databases. Photochem Photobiol 2018; 94: 277–289

[51] Taniguchi M, Lindsey JS. Absorption and fluorescence spectra of organic compounds from 40 sources: Archives, repositories, databases, and literature search engines. SPIE BiOS, 2020, 112560J. doi:10.1117/12.2542859

[52] Taniguchi M, Lindsey JS. Database of absorption and fluorescence spectra of > 300 common compounds for use in PhotochemCAD. Photochem Photobiol 2018; 94: 290–327

[53] Taniguchi M, Bocian DF, Holten D, Lindsey JS. Beyond green with synthetic chlorophylls – Connecting structural features with spectral properties. J Photochem Photobiol C Photochem Rev 2022; 52: 100513

[54] O'Donnell TJ, Gurr JR, Dai J, Taniguchi M, Williams PG, Lindsey JS. Tolyporphins A–R, unusual tetrapyrrole macrocycles in a cyanobacterium from Micronesia, assessed quantitatively from the culture HT-58-2. New J Chem 2021; 45: 11481–11494

[55] Oberhuber M, Berghold J, Kräutler B. Chlorophyll breakdown by a biomimetic route. Angew Chem Int Ed Engl 2008; 47: 3057–3061

[56] Jockusch S, Turro NJ, Banala S, Kräutler B. Photochemical studies of a fluorescent chlorophyll catabolite – source of bright blue fluorescence in plant tissue and efficient sensitizer of singlet oxygen. Photochem Photobiol Sci 2014; 13: 407–411

[57] Moser S, Müller T, Oberhuber M, Kräutler B. Chlorophyll catabolites–chemical and structural footprints of a fascinating biological phenomenon. Eur J Inorg Chem 2009; 2009: 21–31

[58] Li C, Kräutler B. Zn-complex of a natural yellow chlorophyll catabolite. J Porphyr Phthalocyanines 2016; 20: 388–396

[59] Atkinson JH, Atkinson RS, Johnson AW. The structure and reactions of some pyrrolin-2-ones. J Chem Soc 1964: 5999–6009. doi:10.1039/JR9640005999

[60] Struchkova MI, Gusarov AN, Dvoryantseva GG, Evstigneeva RP, Ioslovich NV, Kabankin AS, Kaganskii MM, Landau MA. Electronic spectra and structure of conjugate acids of carbonyl derivatives of pyrrole. Chem Heterocycl Compd 1977; 13: 985–991

[61] Eisner U, Gore PH. 186. The light absorption of pyrroles. Part I. Ultraviolet spectra. J Chem Soc 1958: 922–927. doi:10.1039/JR9580000922

[62] Reddy KR, Lubian E, Pavan MP, Kim HJ, Yang E, Holten D, Lindsey JS. Synthetic bacteriochlorins with integral spiro-piperidine motifs. New J Chem 2013; 37: 1157–1173

[63] Boiadjiev SE, Lightner DA. A water-soluble synthetic bilirubin with carboxyl groups replaced by sulfonyl moieties. Monatsh Chem 2001; 132: 1201–1212

[64] Braslavsky SE, Schneider D, Heihoff K, Nonell S, Aramendia PF, Schaffner K. Phytochrome models. 11. Photophysics and photochemistry of phycocyanobilin dimethyl ester. J Am Chem Soc 1991; 113: 7322–7334

[65] Eichinger D, Falk H. Beiträge zur Chemie der Pyrrolpigmente, 68. Mitt. Zum Kationentransport mit tripyrrinoiden Ionophoren. Monatsh Chem 1987; 118: 91–103

[66] Kräutler B. Breakdown of chlorophyll in higher plants–Phyllobilins as abundant, yet hardly visible signs of ripening, senescence, and cell death. Angew Chem Int Ed Engl 2016; 55: 4882–4907

[67] Kräutler B, Mühlecker W, Anderl M, Gerlach B. Breakdown of chlorophyll: Partial synthesis of a putative intermediary catabolite. Preliminary communication. Helv Chim Acta 1997; 80: 1355–1362

[68] Kuai B, Chen J, Hörtensteiner S. The biochemistry and molecular biology of chlorophyll breakdown. J Exp Bot 2017; 69: 751–767

[69] Hauenstein M, Christ B, Das A, Aubry S, Hörtensteiner S. A role for TIC55 as a hydroxylase of phyllobilins, the products of chlorophyll breakdown during plant senescence. Plant Cell 2016; 28: 2510–2527

[70] Berghold J, Breuker K, Oberhuber M, Hörtensteiner S, Kräutler B. Chlorophyll breakdown in spinach: On the structure of five nonfluorescent chlorophyll catabolites. Photosynth Res 2002; 74: 109–119

[71] Wienkoop S, Baginsky S, Weckwerth W. *Arabidopsis thaliana* as a model organism for plant proteome research. J Proteomics 2010; 73: 2239–2248

[72] Christ B, Hauenstein M, Hörtensteiner S. A liquid chromatography–mass spectrometry platform for the analysis of phyllobilins, the major degradation products of chlorophyll in *Arabidopsis thaliana*. Plant J 2016; 88: 505–518

[73] Kräutler B, Jaun B, Matile P, Bortlik K, Schellenberg M. On the enigma of chlorophyll degradation: The constitution of a secoporphinoid catabolite. Angew Chem Int Ed Engl 1991; 30: 1315–1318

[74] Erhart T, Mittelberger C, Vergeiner C, Scherzer G, Holzner B, Robatscher P, Oberhuber M, Kräutler B. Chlorophyll catabolites in senescent leaves of the plum tree (*Prunus domestica*). Chem Biodivers 2016; 13: 1441–1453

[75] Karg CA, Wang S, Al Danaf N, Pemberton RP, Bernard D, Kretschmer M, Schneider S, Zisis T, Vollmar AM, Lamb DC, Zahler S, Moser S. Tetrapyrrolic pigments from heme- and chlorophyll breakdown are actin-targeting compounds. Angew Chem Int Ed Engl 2021; 60: 22578–22584

[76] Berezin MB, Antina EV, Guseva GB, Kritskaya AY, Semeikin AS. Effect of meso-phenyl substitution on spectral properties, photo- and thermal stability of boron (III) and zinc (II) dipyrrometenates. Inorg Chem Commun 2020; 111: 107611